M.Sc. Thesis

Master of Science in Engineering

DTU Electrical Engineering
Department of Electrical Engineering

Co-ordination of power and natural gas systems under uncertainty

Author:
Álvaro Coll Martínez
student number: s171657

Supervisors:
Anna Schwele
Anubhav Ratha
Jalal Kazempour

Kongens Lyngby, July 2019

DTU Electrical Engineering

Department of Electrical Engineering

Technical University of Denmark

Center of Electric Power and Energy

Elektrovej

Building 325

2800 Kongens Lyngby, Denmark

Phone (+45) 45 25 38 00

elektro@elektro.dtu.dk

www.elektro.dtu.dk

Abstract

The mentality for a greener future with zero emissions is not a blurry thought far away from reality anymore. It is a driver that push people to re-think again the way the resources from the Earth are being used. This paper aims to study a possible transition before it is possible to utilize 100% green energy.

Co-optimization systems are proposed in order to add flexibility, in this case, to the power system and therefore, introduce as much as possible green energy to societies. To be more specific, a co-optimization model where the natural gas is used in the gas-fired power plants to produce the extra energy needed to meet demand is developed. At the same time, minimizing the total system costs of both systems.

Besides, this master thesis also proposes a co-optimization between power and natural gas systems under the uncertainty deriving from renewable energy sources. To do so, the application of chance-constrained programming is a crucial factor. As a result, by assuming known the probability distribution of the total wind power mismatch in the recourse stage, it is possible to quantify the optimal scheduled power to dispatch in the first stage, minimizing the overall system costs and obtaining the maximum wind penetration as possible.

Lastly, several factors are modified to understand, which are the main drivers that affect the most to chance constraints - optimal power flow. The risk level chosen for this new approach and the consequences of varying it is also shown to understand how significant the degree of risk is applied to the chance constraints and how it can affect both variables and total system costs.

List of Figures

List of Tables

Key words

DA: Day Ahead
RT: Real Time
RES: Renewable energy source
DC: Direct current
OPF: Optimal power flow
CC-OPF: Chance constraints - optimal power flow
SOC: Second order cone
CC: Chance constraints
GFPP: Gas-fired power plants
TSO: Transmission system operator
TPP: Thermal power plant
UDI: Unidirectional deterministic implementation
Linepack
QCQP: Quadratically constrained quadratic program

Units

MW: Megawatt
kcf : Kilo cubic feet
rad : Radians
psig : Pound-force per square inch gauge
h : Hours

Nomenclature

Sets

$\mathcal{I}$ Set of dispatchable power plants i.

$\mathcal{C}$ Subset of dispatchable power plants excluding natural gas-fired ones ($\mathcal{C} \subset \mathcal{I}$).

$\mathcal{G}$ Subset of natural gas-fired power plants ($\mathcal{G} \subset \mathcal{I}$).

$\mathcal{J}$ Set of wind power units j.

$\mathcal{T}$ Set of time periods t.

$\mathcal{N}$ Set of electricity network nodes n.

$\mathcal{L}$ Set of electricity transmission lines (n, r), being n the starting node and r the ending one.

$\mathcal{K}$ Set of natural gas supply units k.

$\mathcal{M}$ Set of natural gas network nodes m.

$\mathcal{Z}$ Set of natural gas pipelines (m, u), being m the starting node and u the ending one.

$\mathcal{V}$ Set of fixed pressure points v.

$\mathcal{A}_n^{(.)}$ Set of assets located at electricity network node n.

$\mathcal{A}_m^{(.)}$ Set of assets located at natural gas network node m.

Θ Set of optimization variables.

Variables

$p_{i,t}, w_{j,t}$ Electricity dispatch of units i and j in period t, respectively [MW].

$g_{k,t}$ Natural gas dispatch of unit k in period t [kcf/h].

$\theta_{n,t}$ Voltage angle at node n in period t [rad].

$f_{n,r,t}$ Power flow in line (n,r) in period t [MW].

$pr_{m,t}$ Pressure at node m in period t [psig].

$h_{m,u,t}$ Average mass of natural gas (linepack) in pipeline (m,u) in period t [kcf].

$q^{\text{in/out}}_{m,u,t}$ Inflow/outflow natural gas in pipeline (m,u) in period t [kcf/h].

$q_{m,u,t}$ Natural gas flow in pipeline (m,u) in period t [kcf/h].

$q^{+/-}_{m,u,t}$ Natural gas flow in pipeline (m,u) from node m to u or from node u to m in period t [kcf/h] (depending on the direction of the gas flow).

$y_{m,u,t}$ Binary variable defining the direction of the natural gas flow in pipeline (m,u) in period t, $y_{m,u,t} \in \{0,1\}$.

Parameters

$D^{\text{E}}_{n,t}$ Electricity demand at node n in period t [MW].

$D^{\text{G}}_{m,t}$ Natural gas demand at node m in period t [kcf/h].

C^{E}_{i} Production cost of unit i [$/MWh].

C^{G}_{k} Supply cost of unit k [$/kcf].

$P^{\max}_{i}$ Capacity of dispatchable unit i [MW].

ϕ_i Power conversion factor of natural gas unit $i \in \mathcal{G}$ [kcf/MWh].

$W_{j,t}$ Wind power forecast for unit j in period t [MW].

$G^{\max}_{k}$ Capacity of natural gas unit k [kcf].

$B_{n,r}$ Susceptance of line (n,r) [S].

$F^{\max}_{n,r}$ Transmission capacity of line (n,r) [MW].

$K_{m,u}$ Natural gas flow constant of pipeline (m,u) [kcf/psig].

$S_{m,u}$ Linepack constant of pipeline (m,u) [kcf/(psig h)].

$H^{0}_{m,u}$ Initial linepack in pipeline (m,u) [kcf].

$PR_m^{\min}$ Minimum pressure limit at node m [psig].

$PR_m^{\max}$ Maximum pressure limit at node m [psig].

$\Gamma_{m,u}$ Compressor factor at natural gas pipeline (m, u).

M A sufficiently large constant (i.e. 10,000).

C_{VOLL}^{E} Cost of electricity load shed

C_{VOLL}^{G} Cost of gas load shed

Contents

CHAPTER 1

Introduction

Sustainability, climate change or climate action are some of the many environmental concepts that are slowly raising awareness among society nowadays. Such a mindset have already been considered, years back, as an essential matter to face for some countries, especially the Scandinavian. As a result, it is not a surprise that they are considered as models to follow in terms of harvesting renewable energy. In Denmark, for instance, 40 % of its total power production comes from the wind energy with intentions of increasing it into 50 % by 2020 and become fully sustainable, in all its sectors, by 2050 (chapter 16, [RMS17] and [Pin+17]). However, what is the primary driver in those countries (such as the Scandinavian region) where sustainability has become a must? One theory found in the book *Energy Policy Transition, the perspective of different states* (Introduction, [RMS17]) relates such behaviour with economic development. Such economies that have reached a high level of development compared to the rest of the world seem to push its citizens to think beyond, resulting in a more sensitive society to environmental issues. In consequence, a new mentality that questions how to live under the same living standards without harming planet Earth is emerging and rapidly spreading. The answer? Renewable energy sources (RES) might be a potential one. As a result, new technologies using as primary resources water, wind, sunlight or even the heat of the inside Earth are quickly emerging. Furthermore, there is another aspect, perhaps not as visible, corresponding to industrial strategies. This fundamental matter needs to be well assessed as changing the main sources of energy production may lead to instabilities in the current system, as it was thought in a different perspective by using fossil fuels. Nonetheless, is it possible to become fully sustainable? [RMS17] in its introduction highlights that the way renewable installations are working nowadays, it will not be possible for them to work independently without the back-up of any conventional power generation. The main reason why this is believed is that humans can not control renewable sources; hence, adding uncertainty in any system that relies on them. Energy needs will still be

necessary to supply no matter the shortages of incoming wind or simply rainy days without sunlight. Therefore, until a solution is developed, something needs to be assessed during this *transition* period. Thus, this master thesis, inspired by the paper [Sch+19], tries to generate a full coupling co-optimization between power and natural gas systems under the uncertainty that renewable energies bring into the system. There are several reasons why natural gas is the chosen fossil fuel to give flexibility to the power system. As mentioned in both [Sch+19] and [Pin+17], the entire integrated system in Denmark is operated by the same entity or TSO (Transmission system operator) which is a must for coupled systems. As a result, Energinet.dk is in charge of operating both systems, however, independently. What is more, the co-optimization problem tries to represent an *ideal benchmark*, highlighting all the potential of flexibility that natural gas can provide as a back-up technology, minimizing the overall both system costs [Sch+19] and ensuring not only security of supply but also short-term flexibility [OPM19]. In addition, natural gas (or sometimes known as *blue fuel*, [RMS17]) is considered to be efficient and less polluting to the environment [ULD07], emitting half as much carbon dioxide (CO_2), even though its price might not be lower than other fossil fuels (i.e. coal). By emitting half as much CO_2 compared to other commodities, European countries are also getting closer towards the European goal of cutting emissions by 80-95% [Com12] by 2050. Furthermore, it is also known that gas-fired power plants (GFPP) have higher conversion efficiencies than thermal power plants (TPP), using coal as the main fossil fuel commodity. Numerically speaking, conversion efficiencies in GFPP can raise to 60 %, whereas in coal TPP, plants operate at around 30 %. In monetary terms, GFPP has lower investment costs and a high rate of return of investment compared to other kinds of TPP [Due+14].
To conclude, stochastic programming will also be used in order to account the uncertainty of the renewable sources, adding probabilities of occurrence and hence, allowing some constraints to exceed its boundaries for a specific ϵ times [BCH12]. At the same time, adding the flexibility needed to the power systems by the GFPP. To solve the problems appeared in this document, the Python programming language is used in this master thesis along with Gurobi Optimizer, a commercial optimization solver able to treat from linear programs (LP) to mixed-integer quadratically constrained programming (MIQCP) [Gur19]. Lastly, similarly to the inspiration obtained from [Sch+19], this master thesis also used the python code from [Sch18] as a base for all the applications and approaches used to develop this work.

CHAPTER 2

Literature Review

This chapter aims to show all the knowledge gathered by the material read in order to develop the work that is presented in this master thesis. To start with, one of the main papers used, in which this document is inspired, corresponds to [Sch+19]. The latter gives an idea about how the co-ordination of power and natural gas systems is plausible by using linepack or natural gas storage in the pipelines. As a result, the formulation presented, represents the co-optimization between both systems and highlights also the need of having a single entity in charge of the integrated system, also included in [Pin+17]. However, [Sch+19] focus on a bi-directional flow of the gas through the pipelines, meaning that the flow of the natural gas reacts depending on the needs of each of the nodes. As a result, some equations that determine the direction of the gas through the pipelines were disregard as they were not applied in the model explain in this thesis. Note that this work focuses on the unidirectional flow of the natural gas through the system, as it will be presented in the future sections. It is tried to obtain all the equations and constraints in a SOC form (second-order cone). However, even if this relaxation will be an essential tool to use, [Sch+19] focus on McCormick envelopes, an approach to relax equations with bilinear terms due to the bidirectional flow of the gas [McC76]. As a result, [Che+19] also focuses on the assumption of assuming known the direction of the gas flow, therefore, using a SOC relaxation. However, the paper focus on an enhanced second-order cone, also described in a lecture from The Ohio State University [She+18]. Nevertheless, [She+18] also shows the procedure of using second-order cone relaxation (SOC), the one used in this master thesis. The next step consisted of understanding the concept of linepack, crucial for the development of this co-optimization system. As a result, from [Arv+13] it was understood its ability to store natural gas in the pipelines and displace it from one point to another by applying a differential of pressures.

Chance constraints programming was the central part of the literature review. Two main papers were the fundamentals of all the understanding, explanation and appli-

cation mentioned in this master thesis. [BCH12] Daniel Bienstock et al. in his paper explains in a clear way the reason why chance constraints should be an approach, at least, to be considered when dealing with stochastic programming. Under the uncertainty of the renewables and a society becoming more aware and eager to climate action, more energy from renewable sources is part of the power grid. As a result, chance constraints seeks the most probable realizations under this uncertainty and corrects the possible mismatches through control actions, see also [NS06].
Furthermore, referring to the analytical reformulation of the CC programming, apart from [BCH12] it has also been used another thesis from Line Alnæs Roald, [Roa16]. The latter was used mainly for the power flow programming, as the methodology explained did not have bilinear terms, as the one explained in [BCH12]. As a result, the main contribution of this master thesis is to present an approach to solving the co-ordination between power and natural gas systems, assuming known the direction of the gas flow, under the uncertainty that the wind power brings to the system. Afterwards, the resulting program is applied to a small scale system for further interpretation of the results.

CHAPTER 3

Short-term flexibility

What does exactly mean that natural gas can provide short-term flexibility to the power market? It means that anytime the power market requires electricity to supply the demand because of the lack of enough renewable sources, this resource can be used to obtain the remaining amount. It is true though that nowadays, power systems contain different non-renewable power plants to provide flexibility to the system in case of need, using other fossil fuels (i.e. coal or petroleum) by burning them in thermal power plants. Therefore, why would be interesting to use natural gas as the fossil fuel to provide flexibility? In a transitioning world towards full sustainability, it is also essential to bear in mind which kind of non-renewable fuels impacts the least to the environment. Natural gas results in fewer emissions to the atmosphere of basically all types of pollutants and CO2, compared to the burn of other fossil fuels. In economic terms, natural gas is also a low-cost commodity, compared to crude oil. Even if perhaps coal might be more economical, the difference in its price, nowadays, is slightly different. Furthermore, natural gas possesses the ability to be stored in the pipelines for further usage [Tra+18]. This fact is also known as *linepack* and it plays an essential role in the co-optimization of both power and natural gas systems.

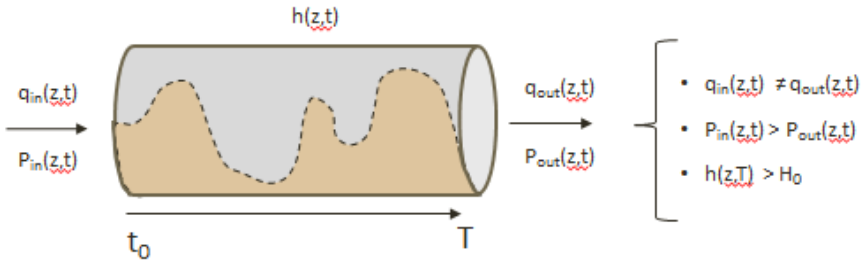

Figure 3.1: Linepack in a pipeline.

3.1 Linepack

Linepack corresponds, as stated previously, to the ability to store natural gas in the pipelines, as stated in [Sch+19]. By applying a differential of pressures between two nodes, part of this natural gas mass can be transported from one point to another [Arv+13].

Figure 3.1 illustrates a pipeline connecting two different nodes. The left side corresponds to the inlet node, while the right side represents the outlet one, showing the direction of displacement of the natural gas. Thus, the inlet pressure per pipeline z at a specific time t is higher than the outlet.

Furthermore, the horizontal arrow under the pipeline reflects the timesteps of the entire time horizon (starting with t_0 until T). Linepack is represented by the variable h(z,t), which corresponds to a specific amount of natural gas stored per pipeline z for one particular period t. As a result, the discontinuous line and the shaded area below it show the amount of linepack for each t, charging or discharging the pipeline depending on the specific needs. Therefore, the amount of gas introduced does not need to be the same amount that exits in the outlet node. Lastly, it is vital to highlight the fact that in the last period T, the amount of linepack in the pipeline must be above or equal a certain level H_0, in order to avoid depletion. Note that the arrow below the pipeline, simply represents the time horizon, highlighting the initial time, corresponding to t_0, and the final to T. In consequence, t_0 does not correspond the left side of the pipe and T the right one, it is just a notation to represent that the amount of natural gas stored will vary for every time step.

CHAPTER 4

Original co-optimization model

This chapter contains all the mathematical formulation to solve the optimization model. The problem in its original form is a mixed-integer program, which is non-convex due to the presence of disjointed feasibility spaces .

The nomenclature for this set of equations is i for the electric nodes, j for the wind farm in its respective electric nodes and the interconnections of power flow, n will refer to the starting node and r to the ending one. On the other hand, k refers to natural gas nodes. However, for gas flow, m will refer to the beginning node and u for the ending one.

As a result, the following set of equations represent the current problem [Sch+19]:

$$\min_{\Theta} \sum_{t\in\mathcal{T}} \Big(\sum_{i\in\mathcal{C}} C_i^{\mathrm{E}}\ p_{i,t} + \sum_{k\in\mathcal{K}} C_k^{\mathrm{G}}\ g_{k,t} \Big) \tag{4.1a}$$

subject to

$$0 \le p_{i,t} \le P_i^{\max}, \forall i, t, \tag{4.1b}$$

$$0 \le w_{j,t} \le W_{j,t}, \forall j, t, \tag{4.1c}$$

$$f_{n,r,t} = B_{n,r}(\theta_{n,t} - \theta_{r,t}), \forall (n,r) \in \mathcal{L}, t \tag{4.1d}$$

$$-F_{n,r}^{\max} \le f_{n,r,t} \le F_{n,r}^{\max}, \forall (n,r) \in \mathcal{L}, t \tag{4.1e}$$

$$-\pi \le \theta_{n,t} \le \pi, \forall n, t,\ \ \theta_{n,t} = 0, \forall n{:}\mathrm{ref}, t \tag{4.1f}$$

$$\sum_{i\in\mathcal{A}_n^I} p_{i,t} + \sum_{j\in\mathcal{A}_n^J} w_{j,t} - \sum_{(n,r)\in\mathcal{L}} f_{n,r,t} = D_{n,t}^{\mathrm{E}}, \forall n, t, \tag{4.1g}$$

$$0 \le g_{k,t} \le G_k^{\max}, \forall k, t, \tag{4.1h}$$

$$PR_m^{\min} \leq pr_{m,t} \leq PR_m^{\max}, \forall m, t, \tag{4.1i}$$

$$pr_{u,t} \leq \Gamma_{m,u}\ pr_{m,t}, \forall (m,u) \in \mathcal{Z}, t, \tag{4.1j}$$

$$q_{m,u,t}|q_{m,u,t}| = K_{m,u}^2(pr_{m,t}^2 - pr_{u,t}^2), \forall (m,u) \in \mathcal{Z}, t, \tag{4.1k}$$

$$q_{m,u,t} = q_{m,u,t}^+ - q_{m,u,t}^-, \forall (m,u) \in \mathcal{Z}, t, \tag{4.1l}$$

$$0 \leq q_{m,u,t}^+ \leq M\ y_{m,u,t}, \forall (m,u) \in \mathcal{Z}, t, \tag{4.1m}$$

$$0 \leq q_{m,u,t}^- \leq M(1 - y_{m,u,t}), \forall (m,u) \in \mathcal{Z}, t, \tag{4.1n}$$

$$q_{m,u,t}^+ = \frac{q_{m,u,t}^{\text{in}} + q_{m,u,t}^{\text{out}}}{2}, \forall (m,u) \in \mathcal{Z}, t, \tag{4.1o}$$

$$q_{m,u,t}^- = \frac{q_{u,m,t}^{\text{in}} + q_{u,m,t}^{\text{out}}}{2}, \forall (m,u) \in \mathcal{Z}, t, \tag{4.1p}$$

$$h_{m,u,t} = S_{m,u}\frac{pr_{m,t} + pr_{u,t}}{2}, \forall (m,u) \in \mathcal{Z}, t, \tag{4.1q}$$

$$h_{m,u,t} = h_{m,u,(t-1)} + q_{m,u,t}^{\text{in}} - q_{m,u,t}^{\text{out}} + q_{u,m,t}^{\text{in}} - q_{u,m,t}^{\text{out}},$$
$$\forall (m,u) \in \mathcal{Z}, t > 1, \tag{4.1r}$$

$$h_{m,u,t} = H_{m,u}^0 + q_{m,u,t}^{\text{in}} - q_{m,u,t}^{\text{out}} + q_{u,m,t}^{\text{in}} - q_{u,m,t}^{\text{out}},$$
$$\forall (m,u) \in \mathcal{Z}, t = 1, \tag{4.1s}$$

$$H_{m,u}^0 \leq h_{m,u,t}, \forall (m,u) \in \mathcal{Z}, t = |\mathcal{T}| \tag{4.1t}$$

$$\sum_{k \in \mathcal{A}_m^K} g_{k,t} - \sum_{i \in \mathcal{A}_m^G} \phi_i\ p_{i,t}$$
$$- \sum_{u:(m,u)\in\mathcal{Z}} (q_{m,u,t}^{\text{in}} - q_{u,m,t}^{\text{out}}) = D_{m,t}^{\text{G}}, \forall m, t, \tag{4.1u}$$

where the set of optimization variables is
$\Theta = \{q_{m,u,t}, y_{m,u,t}, q_{m,u,t}^+, q_{m,u,t}^-, q_{m,u,t}^{\text{in}}, q_{m,u,t}^{\text{out}}, h_{m,u,t}, pr_{m,t}, g_{k,t}, p_{i,t}, w_{j,t}, \theta_{n,t}, f_{n,r,t}\}$.

The objective of this problem is to minimize the total costs along with finding the optimal power and natural gas dispatch. Equation 4.1a reflects the objective function of this co-optimization problem, minimizing the total costs over the time horizon. Constraints 4.1b and 4.1c limit the maximum production for both electricity obtained by conventional power plant generation and wind farms. Equation 4.1d refers to the amount of power that flows from one node to another. In case of a negative value, it means that the flow is from node r to node n, instead of going from node n to node r. However, line transmissions can only flow a limited amount of power, and thus, 4.1e sets their maximum capacities (in both directions). The same occurs with the voltage angles; their maximum and the minimum value is defined by constraint 4.1f.

Moreover, one of the nodes will be considered as a reference node, fixing its voltage angle to 0. In this specific problem, the electric node i1 is set as the reference and thus, $\theta_{n=n1,t} = 0$. Equation 4.1g sets the power balancing constraint, which assures that the demand is always met. It states that all the electricity generated by both wind farms and conventional generators in each electric node; plus the difference between the power flow received and sent, must be equal to the demand of electricity of that specific electric node; for all nodes and time steps over the 24 hour time horizon.
On the other hand, the following set of equations 4.1h-4.1u will refer to the natural gas constraints. As with the electricity generation, equation 4.1h fixes the maximum production of natural gas in each of the nodes (in case of existing a natural gas supplier). Furthermore, in order to be able to flow the gas from one node to another, the pressure of the nodes plays an important role. Therefore, minimum and maximum levels are defined for each of the gas nodes for the entire 24h time horizon, as shown in equation 4.1i. Besides, constraint 4.1j specifies the maximum value that the receiving natural gas node can obtain, as the gas displaces from node m to node u. With the unknown direction of the gas flow, a quadratic constraint is considered in the set of equations, 4.1k. As a result, in order to determine the direction of the gas flow, equations 4.1l, 4.1m, 4.1n, 4.1o and 4.1p will be also required. The piecewise quadratic non-convex constraint, known as Weymouth equation [MBT09], showed in 4.1k, illustrates that the steady-state gas flow between nodes m and u is equal to a parameter ($K^2_{m,u}$) that relates the gas flow with the difference of the squared pressures in adjacent nodes. This ($K^2_{m,u}$) constant is a physical property of the pipeline. Also, the absolute value in the Weymouth equation shows the direction of the natural gas flow, positive if it goes from node m to u or negative if it is the other way around. By using a binary variable $y_{m,u,t}$, the natural gas flow in each pipeline is decomposed in two non-negative variables $q^+_{m,u,t}$ and $q^-_{m,u,t}$ (equations 4.1m and 4.1n). As a result, depending on the value of the binary variable, one of the two non-negative variables will result 0, defining the value of $q_{m,u,t}$ in equation 4.1l. Lastly, equations 4.1o and 4.1p will quantify the variables $q^+_{m,u,t}$ and $q^-_{m,u,t}$ as the average of inflow and outflow, in case their values are different than 0. The following figure illustrates the dynamics of the bi-directional flow:

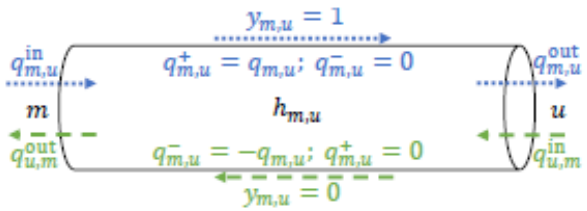

Figure 4.1: Bi-directional flow along a pipeline (time index t is dropped for notational clarity.

The next set of equations (from 4.1q to 4.1s) refer to the *linepack*. The way linepack is defined corresponds to equation 4.1q, which depends on the average pressure between the two adjacent nodes multiplied by the linepack constant of the pipeline $S_{m,u}$. In addition, for every time period, the new linepack for period t will also be formed by the linepack from the previous period (t-1) plus the inflow of natural gas from the node m minus the outflow of natural gas at node u (equation 4.1r). Apart from that, when t=1, the linepack constraint will be the same except that the previous linepack is replaced by an initial value stated as an input (equation 4.1s). At the same time, in order to avoid the depletion in the natural gas network, a minimum linepack will be imposed at the end of the time period (T), in this case, t=24 (equation 4.1t). Finally, the last equation is the coupling constraint. It imposes the natural gas balance in each node, coupling also both power and natural gas systems through the fuel consumption of the natural gas-fired power plants (NGFPP). The first term represents the total supply of natural gas in node k through the set of natural gas supply units located at the same natural gas node k. Then, the amount used in gas-fired power plants to produce power, multiplied by the conversion factor of the natural gas units through the subset of natural gas-fired power plants in node k is subtracted. Finally, the subtraction of the gas sent to another node plus the gas received, both in and from node k, must be equal to the natural gas demand (equation 4.1u).

CHAPTER 5

Unidirectional deterministic implementation.

This section focus on the co-optimization model formulated in chapter 3 with some modifications and assumptions. Furthermore, it also highlights the main differences in the model when linepack is used. It also shows how the model behaves with a deterministic implementation or, in other words, dispatching the optimal quantities without uncertainty (i.e. risk-free).

5.1 One stage programming

5.1.1 Assumptions

Firstly, it has been considered a deterministic implementation, not taking into account the possible scenarios due to the uncertainty of the renewables (wind in this specific case). Thus, the predictions collected by the forecast are treated as accurate information with no need for adjustments. Moreover, in order to simplify the model, it has been assumed that the direction of the gas flow is known. As a result, only natural gas can be flown from gas nodes k3 to k1 and from k1 to k2 preventing any other possibility. Hence, the mathematical model will be considerably simplified. In addition, neither power nor gas losses have been considered through the transmission lines connecting the electric nodes or the pipelines, connecting the gas nodes. As a

result, the final objective value will not contain extra cost due to losses. Lastly, a simple DC formulation of the power flow is also used since an accurate representation of the natural gas flow dynamics is sought.

5.1.2 Simplified mathematical model without linepack

The following set of equations represent the simplified mathematical model after applying all the assumptions from the previous section:

$$\min_{\Theta} \sum_{t\in\mathcal{T}} \Big(\sum_{i\in\mathcal{C}} C_i^{\mathrm{E}}\ p_{i,t} + \sum_{k\in\mathcal{K}} C_k^{\mathrm{G}}\ g_{k,t} \Big) \tag{5.1a}$$

subject to

$$0 \le p_{i,t} \le P_i^{\max}, \forall i,t, \tag{5.1b}$$

$$0 \le w_{j,t} \le W_{j,t}, \forall j,t, \tag{5.1c}$$

$$f_{n,r,t} = B_{n,r}(\theta_{n,t} - \theta_{r,t}), \forall (n,r) \in \mathcal{L}, t \tag{5.1d}$$

$$-F_{n,r}^{\max} \le f_{n,r,t} \le F_{n,r}^{\max}, \forall (n,r) \in \mathcal{L}, t \tag{5.1e}$$

$$-\pi \le \theta_{n,t} \le \pi, \forall n,t,\ \ \theta_{n,t} = 0, \forall n{:}\mathrm{ref}, t \tag{5.1f}$$

$$\sum_{i\in\mathcal{A}_n^I} p_{i,t} + \sum_{j\in\mathcal{A}_n^J} w_{j,t} - \sum_{(n,r)\in\mathcal{L}} f_{n,r,t} = D_{n,t}^{\mathrm{E}}, \forall n,t, \tag{5.1g}$$

$$0 \le g_{k,t} \le G_k^{\max}, \forall k,t, \tag{5.1h}$$

$$PR_m^{\min} \le pr_{m,t} \le PR_m^{\max}, \forall m,t, \tag{5.1i}$$

$$pr_{u,t} \le \Gamma_{m,u}\ pr_{m,t}, \forall (m,u) \in \mathcal{Z}, t, \tag{5.1j}$$

$$q_{m,u,t}^2 = K_{m,u}^2 (pr_{m,t}^2 - pr_{u,t}^2), \forall (m,u) \in \mathcal{Z}, t, \tag{5.1k}$$

$$0 \le q_{m,u,t}, q_{m,u,t}^{\mathrm{in}}, q_{m,u,t}^{\mathrm{out}}, \forall (m,u) \in Z, t \tag{5.1l}$$

$$q_{m,u,t} = \frac{q_{m,u,t}^{\mathrm{in}} + q_{m,u,t}^{\mathrm{out}}}{2}, \forall (m,u) \in \mathcal{Z}, t, \tag{5.1m}$$

$$q_{m,u,t}^{\mathrm{in}} = q_{m,u,t}^{\mathrm{out}} \forall (m,u) \in Z, t \tag{5.1n}$$

$$\sum_{k\in\mathcal{A}_m^K} g_{k,t} - \sum_{i\in\mathcal{A}_m^G} \phi_i\ p_{i,t} - \sum_{u:(m,u)\in\mathcal{Z}} (q_{m,u,t}^{\mathrm{in}} - q_{u,m,t}^{\mathrm{out}}) = D_{m,t}^{\mathrm{G}}, \forall m,t, \tag{5.1o}$$

where the set of optimization variables is
$\Theta = \{q_{m,u,t}, q_{m,u,t}^{\mathrm{in}}, q_{m,u,t}^{\mathrm{out}}, pr_{m,t}, g_{k,t}, p_{i,t}, w_{j,t}, \theta_{n,t}, f_{n,r,t}\}$.

When assuming known direction of the gas flow, the absolute value in equation 4.1k is removed, resulting $q^2_{m,u,t}$. Furthermore, there is no need to include the binary variable which, as stated previously, was helping to define the direction of the flow. Thus, equation 4.1m and 4.1n are also removed. Equations 4.1o and 4.1p will turn into one single equation quantifying the value of the gas flow as the average of inflow and outflow in the known direction. However, as there is no possible natural gas storage in the pipelines, all the amount of gas introduced in a node will be exiting in its adjacent node. This is shown in equation 8.1. Besides, equation 4.1l will no longer be needed, as it is assumed that the direction of the gas flow is known. Thus, $q_{m,u,t}$ will be directly the amount introduced in the pipeline. Nevertheless, it is important to highlight that $q_{m,u,t}$ will be a non-negative variable; therefore, a new constraint must be added, forcing the non-negativity of the gas flow. Lastly, all linepack equations (4.1q - 4.1t) are removed from the co-optimization model.

5.1.3 Simplified mathematical model with linepack

When linepack is taken into consideration for the formulation, the following set of constraints describe the system:

$$\min_{\Theta} \sum_{t\in\mathcal{T}} \Big(\sum_{i\in\mathcal{C}} C^{\mathrm{E}}_i \; p_{i,t} + \sum_{k\in\mathcal{K}} C^{\mathrm{G}}_k \; g_{k,t} \Big) \tag{5.2a}$$

subject to

$$0 \le p_{i,t} \le P^{\max}_i, \forall i, t, \tag{5.2b}$$

$$0 \le w_{j,t} \le W_{j,t}, \forall j, t, \tag{5.2c}$$

$$f_{n,r,t} = B_{n,r}(\theta_{n,t} - \theta_{r,t}), \forall (n,r) \in \mathcal{L}, t \tag{5.2d}$$

$$-F^{\max}_{n,r} \le f_{n,r,t} \le F^{\max}_{n,r}, \forall (n,r) \in \mathcal{L}, t \tag{5.2e}$$

$$-\pi \le \theta_{n,t} \le \pi, \forall n, t, \;\; \theta_{n,t} = 0, \forall n{:}\mathrm{ref}, t \tag{5.2f}$$

$$\sum_{i\in\mathcal{A}^I_n} p_{i,t} + \sum_{j\in\mathcal{A}^J_n} w_{j,t} - \sum_{(n,r)\in\mathcal{L}} f_{n,r,t} = D^{\mathrm{E}}_{n,t}, \forall n, t, \tag{5.2g}$$

$$0 \le g_{k,t} \le G^{\max}_k, \forall k, t, \tag{5.2h}$$

$$PR^{\min}_m \le pr_{m,t} \le PR^{\max}_m, \forall m, t, \tag{5.2i}$$

$$pr_{u,t} \le \Gamma_{m,u} \; pr_{m,t}, \forall (m,u) \in \mathcal{Z}, t, \tag{5.2j}$$

$$q^2_{m,u,t} = K^2_{m,u}(pr^2_{m,t} - pr^2_{u,t}), \forall (m,u) \in \mathcal{Z}, t, \tag{5.2k}$$

$$0 \leq q_{m,u,t}, q^{\text{in}}_{m,u,t}, q^{\text{out}}_{m,u,t}, \forall (m,u) \in Z, t \tag{5.2l}$$

$$q_{m,u,t} = \frac{q^{\text{in}}_{m,u,t} + q^{\text{out}}_{m,u,t}}{2}, \forall (m,u) \in \mathcal{Z}, t, \tag{5.2m}$$

$$h_{m,u,t} = S_{m,u} \frac{pr_{m,t} + pr_{u,t}}{2}, \forall (m,u) \in \mathcal{Z}, t, \tag{5.2n}$$

$$h_{m,u,t} = h_{m,u,(t-1)} + q^{\text{in}}_{m,u,t} - q^{\text{out}}_{m,u,t}, \forall (m,u) \in \mathcal{Z}, t > 1, \tag{5.2o}$$

$$h_{m,u,t} = H^0_{m,u} + q^{\text{in}}_{m,u,t} - q^{\text{out}}_{m,u,t}, \forall (m,u) \in \mathcal{Z}, t = 1, \tag{5.2p}$$

$$H^0_{m,u} \leq h_{m,u,t}, \forall (m,u) \in \mathcal{Z}, t = |\mathcal{T}| \tag{5.2q}$$

$$\sum_{k \in \mathcal{A}^K_m} g_{k,t} - \sum_{i \in \mathcal{A}^G_m} \phi_i \; p_{i,t} - \sum_{u:(m,u) \in \mathcal{Z}} (q^{\text{in}}_{m,u,t} - q^{\text{out}}_{u,m,t}) = D^{\text{G}}_{m,t}, \forall m, t, \tag{5.2r}$$

where the set of optimization variables is
$\Theta = \{q_{m,u,t}, q^{\text{in}}_{m,u,t}, q^{\text{out}}_{m,u,t}, h_{m,u,t}, pr_{m,t}, g_{k,t}, p_{i,t}, w_{j,t}, \theta_{n,t}, f_{n,r,t}\}$.

A couple of changes need to be highlighted when describing the model with linepack. It is true though that most of model coincide with the one without natural gas storage. However, equation 5.1n does not apply as the amount of natural gas introduced in the pipeline does not need to match the outlet amount. With linepack, another variable is added to the system. Therefore, gas can be kept in the pipelines. As a result, equation 5.2n determines the average mass in each pipeline. Furthermore, mass conservation in each pipeline is enforced by equation 5.2o. Moreover, two more constraints representing the first time step (equation 5.2p) and the minimum remaining amount at the end of the last period T to avoid depletion (equation 5.2q) need to be also added.

5.1.4 Second-order cone (SOC) relaxation

However, after describing both models with and without linepack, there is still something to accomplish. All sets of equations described in this chapter have the same constraint, the Weymouth equation 5.1k. This equation shows that the constraint is still in a quadratic form. Therefore, the problem is non-convex, and in consequence, the solution obtained may not be optimal. The reason why this happens is that when the problem is non-convex, it appears both local and global minimum/-maximum. In consequence, it is possible that the problem finds a solution located

in the local minimum/maximum and not in the global, as quadratic equations have more than one solution [Bee17]. Hence, this is the main reason why convexification techniques need to be applied to the Weymouth equation in order to transform the problem into convex and assure optimality in the solution found. However, what is precisely a second-order cone problem? As it is mentioned in [AG03], a second-order cone programming (SOCP) corresponds to convex optimization problems where a linear function is minimized over the intersection of an affine linear manifold with the Cartesian product of the second-order cones. As a result, in this master thesis, the objective function is already linear, but one equation is quadratic. Quadratically constrained quadratic programs (QCQP) can be transformed as the minimization of a linear function subject to convex quadratic constraints[AG03]:

$$\min_{\Theta} \; ax + b \tag{5.3a}$$

subject to

$$c_i x^2 + d_i x + e \leq 0, \forall i, \tag{5.3b}$$

where the set of optimization variables is
$\Theta = \{x\}$.
Where a, b, c_i, d_i and e represent parameters of the quadratically constrained quadratic program (QCQP). As a result, the same procedure can be applied in the co-optimization model of this master thesis, obtaining the following second-order cone (SOC) relaxation to the quadratic constraint:

$$q^2_{m,u,t} \leq K^2_{m,u}(pr^2_{m,t} - pr^2_{u,t}), \quad \forall (m,u) \in \mathcal{Z}, t \tag{5.4a}$$

From now on, the co-optimization problem can be treated as a convex program. However, it is crucial to bear in mind that the actual constraint corresponds to an equality constraint, not inequality. Thus, solution checks will be needed in order to assure that the problem is behaving as it will do in reality.

5.2 Two stage programming

This section contains a new aspect that was not considered in 1 stage deterministic section, a recourse stage. As a result, the model will contain first-stage decision variables in the presence of variations in the recourse stage. Besides, in the second stage, the actual value of the future realizations will be known, and thus, corrective actions and recourse decisions can be taken. First-stage decisions are, in consequence, optimized by considering their future effects. These future effects are computed in a recourse function, which measures the expected value of the decision made in the first stage. For clarity of notation, the values in the first-stage will correspond to the day ahead (DA) decisions, and real-time (RT) will represent the recursive or second stage variables.

5.2.1 Assumptions

The assumptions considered in this section are similar to the ones considered in the deterministic case. Two-stage programming, however, focuses on a deterministic implementation where a recourse stage is present, contributing as adjustments for the first stage decisions. Besides, this section will also assume that the direction of the gas flow is known, from node k3 to k1 and from k1 to k2. Furthermore, it is also assumed no losses in neither transmission lines nor pipelines. A DC formulation of the power flow and the presence of linepack in the pipelines will be considered for this section. Finally, all generators are flexible in real-time, and they can, therefore, adjust their production in real-time compared to what they were supposed to dispatch in DA.

5.2.2 Mathematical formulation

The following set of equations represents the 2 stage program:

$$\min_{\Theta} \sum_{t\in\mathcal{T}} \Big(\sum_{i\in\mathcal{C}} C_i^{\mathrm{E}}\ p_{i,t}^{DA} + \sum_{k\in\mathcal{K}} C_k^{\mathrm{G}}\ g_{k,t}^{DA} \Big) + \sum_{t\in\mathcal{T}} \Bigg[\Big(\sum_{i\in\mathcal{C}} C_i^{\mathrm{E}}\ p_{i,t}^{RT} + \sum_{n\in\mathcal{N}} C_{VOLL}^{E} LS_{n,t}^{E} \Big) + + \sum_{k\in\mathcal{K}} \Big(C_k^{\mathrm{G}}\ g_{k,t}^{RT} + \sum_{m\in\mathcal{M}} C_{VOLL}^{G} LS_{m,t}^{G} \Big) \Bigg] \tag{5.5a}$$

subject to

Day-Ahead constraints

$$0 \leq p_{i,t}^{DA} \leq P_i^{\max}, \forall i, t, \tag{5.5b}$$

$$0 \leq w_{j,t}^{DA} \leq W_{j,t}, \forall j, t, \tag{5.5c}$$

$$f_{n,r,t}^{DA} = B_{n,r}(\theta_{n,t}^{DA} - \theta_{r,t}^{DA}), \forall (n,r) \in \mathcal{L}, t \tag{5.5d}$$

$$-F_{n,r}^{\max} \leq f_{n,r,t}^{DA} \leq F_{n,r}^{\max}, \forall (n,r) \in \mathcal{L}, t \tag{5.5e}$$

$$-\pi \leq \theta_{n,t}^{DA} \leq \pi, \forall n, t, \;\; \theta_{n,t}^{DA} = 0, \forall n{:}\text{ref}, t \tag{5.5f}$$

$$\sum_{i \in \mathcal{A}_n^I} p_{i,t}^{DA} + \sum_{j \in \mathcal{A}_n^J} w_{j,t}^{DA} - \sum_{(n,r) \in \mathcal{L}} f_{n,r,t}^{DA} = D_{n,t}^{\mathrm{E}}, \forall n, t, \tag{5.5g}$$

$$0 \leq g_{k,t}^{DA} \leq G_k^{\max}, \forall k, t, \tag{5.5h}$$

$$PR_m^{\min} \leq pr_{m,t}^{DA} \leq PR_m^{\max}, \forall m, t, \tag{5.5i}$$

$$pr_{u,t}^{DA} \leq \Gamma_{m,u}\, pr_{m,t}^{DA}, \forall (m,u) \in \mathcal{Z}, t, \tag{5.5j}$$

$$q_{m,u,t}^{2DA} \leq K_{m,u}^2 (pr_{m,t}^{2DA} - pr_{u,t}^{2DA}), \forall (m,u) \in \mathcal{Z}, t, \tag{5.5k}$$

$$0 \leq q_{m,u,t}^{DA}, q_{m,u,t}^{\text{in DA}}, q_{m,u,t}^{\text{out DA}}, \forall (m,u) \in Z, t \tag{5.5l}$$

$$q_{m,u,t}^{DA} = \frac{q_{m,u,t}^{\text{in DA}} + q_{m,u,t}^{\text{out DA}}}{2}, \forall (m,u) \in \mathcal{Z}, t, \tag{5.5m}$$

$$h_{m,u,t}^{DA} = S_{m,u} \frac{pr_{m,t}^{DA} + pr_{u,t}^{DA}}{2}, \forall (m,u) \in \mathcal{Z}, t, \tag{5.5n}$$

$$h_{m,u,t}^{DA} = h_{m,u,(t-1)}^{DA} + q_{m,u,t}^{\text{in DA}} - q_{m,u,t}^{\text{out DA}}, \forall (m,u) \in \mathcal{Z}, t > 1, \tag{5.5o}$$

$$h_{m,u,t}^{DA} = H_{m,u}^0 + q_{m,u,t}^{\text{in DA}} - q_{m,u,t}^{\text{out DA}}, \forall (m,u) \in \mathcal{Z}, t = 1, \tag{5.5p}$$

$$H_{m,u}^0 \leq h_{m,u,T}^{DA}, \forall (m,u) \in \mathcal{Z}, t = |\mathcal{T}| \tag{5.5q}$$

$$\sum_{k \in \mathcal{A}_m^K} g_{k,t}^{DA} - \sum_{i \in \mathcal{A}_m^G} \phi_i \; p_{i,t}^{DA} - \sum_{u:(m,u) \in \mathcal{Z}} (q_{m,u,t}^{\text{in DA}} - q_{u,m,t}^{\text{out DA}}) = D_{m,t}^{\mathrm{G}}, \forall m, t, \tag{5.5r}$$

Real-Time constraints

$$0 \leq p_{i,t}^{DA} + p_{i,t}^{RT} \leq P_i^{\max}, \forall i, t, \tag{5.6a}$$

$$0 \leq w_{j,t}^{RT} \leq W_{j,t}, \forall j, t, \tag{5.6b}$$

$$f_{n,r,t}^{RT} = B_{n,r}(\theta_{n,t}^{RT} - \theta_{r,t}^{RT}), \forall (n,r) \in \mathcal{L}, t \tag{5.6c}$$

$$-F_{n,r}^{\max} \leq f_{n,r,t}^{RT} \leq F_{n,r}^{\max}, \forall (n,r) \in \mathcal{L}, t \tag{5.6d}$$

$$-\pi \leq \theta^{RT}_{n,t} \leq \pi, \forall n,t, \;\; \theta^{RT}_{n,t} = 0, \forall n\text{:ref},t \tag{5.6e}$$

$$\sum_{i\in\mathcal{A}^I_n} p^{RT}_{i,t} + \sum_{j\in\mathcal{A}^J_n} (w^{RT}_{j,t} - w^{DA}_{j,t}) - \sum_{(n,r)\in\mathcal{L}} (f^{RT}_{n,r,t} - f^{DA}_{n,r,t}) + LS^E_{n,t} = 0, \forall n,t, \tag{5.6f}$$

$$0 \leq LS^E_{n,t} \leq D^E_{n,t} \forall n,t \tag{5.6g}$$

$$0 \leq g^{DA}_{k,t} + g^{RT}_{k,t} \leq G^{\max}_k, \forall k,t, \tag{5.6h}$$

$$PR^{\min}_m \leq pr^{RT}_{m,t} \leq PR^{\max}_m, \forall m,t, \tag{5.6i}$$

$$pr^{RT}_{u,t} \leq \Gamma_{m,u}\ pr^{RT}_{m,t}, \forall (m,u) \in \mathcal{Z}, t, \tag{5.6j}$$

$$q^{2RT}_{m,u,t} \leq K^2_{m,u}(pr^{2RT}_{m,t} - pr^{2RT}_{u,t}), \forall (m,u) \in \mathcal{Z}, t, \tag{5.6k}$$

$$0 \leq q^{RT}_{m,u,t}, q^{\text{in RT}}_{m,u,t}, q^{\text{out RT}}_{m,u,t}, \forall (m,u) \in Z, t \tag{5.6l}$$

$$q^{RT}_{m,u,t} = \frac{q^{\text{in RT}}_{m,u,t} + q^{\text{out RT}}_{m,u,t}}{2}, \forall (m,u) \in \mathcal{Z}, t, \tag{5.6m}$$

$$h^{RT}_{m,u,t} = S_{m,u} \frac{pr^{RT}_{m,t} + pr^{RT}_{u,t}}{2}, \forall (m,u) \in \mathcal{Z}, t, \tag{5.6n}$$

$$h^{RT}_{m,u,t} = h^{RT}_{m,u,(t-1)} + q^{\text{in RT}}_{m,u,t} - q^{\text{out RT}}_{m,u,t}, \forall (m,u) \in \mathcal{Z}, t > 1, \tag{5.6o}$$

$$h^{RT}_{m,u,t} = H^0_{m,u} + q^{\text{in RT}}_{m,u,t} - q^{\text{out RT}}_{m,u,t}, \forall (m,u) \in \mathcal{Z}, t = 1, \tag{5.6p}$$

$$H^0_{m,u} \leq h^{RT}_{m,u,T}, \forall (m,u) \in \mathcal{Z}, t = |\mathcal{T}| \tag{5.6q}$$

$$\sum_{k\in\mathcal{A}^K_m} g^{RT}_{k,t} - \sum_{i\in\mathcal{A}^G_m} \phi_i\ p^{RT}_{i,t} - \sum_{u:(m,u)\in\mathcal{Z}} \Big((q^{\text{in RT}}_{m,u,t} - q^{\text{out RT}}_{u,m,t}) - (q^{\text{in DA}}_{m,u,t} - q^{\text{out DA}}_{u,m,t}) \Big) + LS^G_{m,t} = 0, \forall m,t, \tag{5.6r}$$

$$0 \leq LS^G_{m,t} \leq D^G_{m,t} \forall n,t \tag{5.6s}$$

where the set of optimization variables is
$\Theta = \{q^{DA}_{m,u,t}, q^{RT}_{m,u,t}, q^{\text{in DA}}_{m,u,t}, q^{\text{in RT}}_{m,u,t} q^{\text{out DA}}_{m,u,t}, q^{\text{out RT}}_{m,u,t} h^{DA}_{m,u,t}, h^{RT}_{m,u,t}, pr^{DA}_{m,t}, pr^{RT}_{m,t}, g^{DA}_{k,t}, g^{RT}_{k,t}$, $p^{DA}_{i,t}, p^{RT}_{i,t}, w^{DA}_{j,t}, w^{RT}_{j,t}, \theta^{DA}_{n,t}, \theta^{RT}_{n,t}, f^{DA}_{n,r,t}, f^{RT}_{n,r,t}, LS^G_{m,t}, LS^E_{n,t}\}$.
It is essential to highlight a few aspects of this set of equations. First of all, the objective function corresponds to all the costs in day-ahead and in real-time. The latter consider all the power and gas adjustments and also all the missing quantity to meet the demand in both power and natural gas, the load shed. In order to minimize the total costs, the cost of the load shed is high enough compared to the others. Thus, when optimizing, the value will be the lowest as possible. The day-ahead constraints are the same set of equations as the ones explained in the 1 stage programming chapter. On the other hand, both productions of power and natural gas in real-time correspond to adjustments of their day-ahead variables. All the rest of the variables

show the final value obtained in real-time. Also, the power balancing equation 5.6f states that all the power production adjustments by conventional power plants, wind farms, power flow and the load shed should be equal to 0. Hence, it is necessary to account the difference between the values in real-time and day-ahead, for both wind production and power flow.
Moreover, a new variable representing the load shed is also added in case it is not possible to meet the demand.
Similarly, the gas coupling constraint represented by equation 5.6r, assures that all the adjustments plus the gas load shed equals to 0. The difference between the variation in the gas production (in respect of its day-ahead variable) and both the amount of natural gas used to produce power and the gas flown between nodes must be 0. The variation in gas flow is accounted for the difference between the inlet and outlet amount and compared to the variation in day-ahead. Finally, another load shed variable to consider the missing gas quantity to meet the demand is also introduced. In addition, the rest of the constraints in real-time are the same as the ones described in previous chapters. However, the only difference is that both equations 5.6a and 5.6h represent capacity constraints. As mentioned previously, the total quantity produced in both day-ahead and real-time should not exceed the maximum capacity, as both RT variables represent adjustments. Lastly, two new constraints are introduced, representing the maximum and minimum values of both power and gas load shed (shown in equations 5.6g and 5.6s).

CHAPTER 6

Chance constrained programming

Nowadays, many countries in the globe have different renewable policies and targets to become fully sustainable. Denmark, for example, obtains around 40 % of its total electricity from the wind energy with plans to increase the number to 50 % by 2020 and have 100% renewable electricity by 2050 (chapter 16, [RMS17]). This fact, however, brings many technical challenges with it as the introduction of renewables into the power system brings with it uncertainty. Nevertheless, what is the meaning of uncertainty, and why is that such a problem to solve? Going back in time to where the grids were built, the infrastructure considered deterministic amounts of power with basically no uncertainty. In other words, if a conventional power plant in node A needs to flow power to node B, the capacity of the transmission line will be built according to the characteristics of the plant and demand in both nodes A and B.
Large-scale introduction of renewables brings with it the risk of large, random variability, leading to a situation that the actual grid is not developed to accommodate [BCH12]. As a result, recourse actions in real-time can lead to producing amounts of power that exceeds lines ratings and thus, the lines become more likely to trip. Moreover, if several lines trip, the entire grid becomes more unstable and can experience a cascading failure. The non-deterministic behaviour of renewables, in this specific case, the wind, makes it possible to assess the risk of overload lines in terms of probabilities, relying on stochastic optimization. Therefore, this section proposes a new method that searches for the most probable realizations of line and generator's production overloads under renewables and corrects such situations through control actions. Chance-constrained optimization focuses on solving such problems under uncertainty. Given a certain probability of occurrence for a particular event, (with

a risk parameter); it is possible to minimize the average cost of generation over random power injections. Moreover, it also assures that generators can compensate in real-time renewables fluctuations, guaranteeing with a low probability that a line will exceed its rating [BCH12]. At the same time, productions by generators will exceed, with low probability, their maximum capacity.

6.1 Methodology

In the previous chapter, a two-stage problem was introduced considering known the amount of wind, accounting; therefore, the real value of the power produced by the wind farms. However, this is an ideal situation as, in real life, the exact amount is unknown beforehand. As stated previously, CC-OPF (chance constraints - optimal power flow) minimize the average cost of generation over the random power injections. In order to do that, the probability of meeting a specific constraint is above a certain level of ϵ. However, two different approaches can be used: single and joint constraints.
In single chance constraints, a certain probability can be applied to each of the inequality constraints of the model. As a result, each of the individual constraints can be transformed analytically.

$$\mathbb{P}\Big(p_{i,t}^{DA} + p_{i,t}^{RT} \leq P^{max}\Big) \geq 1 - \epsilon, \forall i, t \tag{6.1a}$$

Equation 6.1 shows how chance constraints are applied to a recourse action that depends on the uncertainty. The variables shown in equation 6.1 illustrate both first and recourse stage. As a result, $p_{i,t}^{DA}$ represents the amount accounted in the first stage while the other variable, $p_{i,t}^{RT}$, refers to the adjustments produced in the recourse stage. In this master thesis, the first stage variables will also be named as *Day Ahead* (DA) since they work with the forecasted wind values. On the other hand, the *Real Time* (RT) variables account for all the adjustments considered after obtaining the real amount of wind power.
By considering a specific risk parameter (ϵ), the probability of meeting that constraint is 1-ϵ. As a result, with single chance constraints, there will be a total set of $|I| \cdot |T|$ equations, each of them following their probability of occurrence independently.
On the other hand, the main difference with joint chance constraints is that all the

equations need to be fulfilled simultaneously. As a result, a specific solution cannot be obtained since the calculation of a joint probability of multivariate uncertain variables is needed. This is the main drawback of joint chance constraints that it is challenging to compute the probability value [MP06]. As a result, this chapter applies single chance constraints. The following equation represents the joint chance constraint:

$$\mathbb{P}\left(p_{i,t}^{DA} + p_{i,t}^{RT} \leq P^{max}, \forall i, t\right) \geq 1 - \epsilon \tag{6.2a}$$

Equation 6.2a shows how all the original constraints act as a whole, meaning that they are reformulated as one single chance constraint with the probability of meeting all the constraints of 1-ϵ.

6.2 Application in the co-optimization model

When applying chance constraints to a model, it is essential to identify the uncertainty sources. In this specific model, the uncertain source is the wind. As a result, it is possible to, therefore model the quantity of power obtained by [Roa16]:

$$\tilde{u} = u_f + \delta u \tag{6.3a}$$

Where $\tilde{u}$ represents the uncertainty sources, u_f is the sum of forecasted production and δu is a random fluctuation where usually its probability distribution is unknown. However, it is assumed that this random fluctuation will follow a normal distribution with mean μ and standard deviation σ. A non-zero mean μ is considered since the forecasts are not necessarily based on the expectation of $\tilde{u}$. Therefore, the total amount obtained of $\tilde{u}$ can also be represented as:

$$\tilde{u} = u_f + \mu + \omega \tag{6.4a}$$

However, with all the above information, equation 6.4 can be rewritten in terms of the expected power production and a zero-mean fluctuating component:

$$u' = u_f + \mu \tag{6.5a}$$

$$\tilde{u} = u' + \omega \tag{6.5b}$$

Where ω represents the fluctuating component per generator. As a result, assuming known both μ and ω by estimations based on historical data, the total power mismatch Ω can also be calculated by:

$$\Omega = \sum_{j \in \mathcal{A}_n^J} (\omega_j) \tag{6.6a}$$

Where Ω is assumed to follow a Gaussian distribution N(μ'= 0,σ). Thus, this σ can be estimated by the following formula:

$$\sigma_\Omega = \sqrt{1_{1,m} \Sigma_W 1_{1,m}^T} \tag{6.7a}$$

Where $1_{1,m} \in R^{1xm}$ is a row of vectors of 1 with dimension m. On the other hand, Σ_W corresponds to the matrix of covariances with 0 except the diagonal, that contains the fluctuation components (ω_j^2) of each wind power generator. When forecast errors occur, an adjustment in the controllable generation must balance the total power mismatch Ω. This amount of requested up/downregulation is proportional to the total power mismatch with the opposite sign:

$$\tilde{p}_G(\Omega) = p_G - \alpha\Omega \tag{6.8a}$$

Where $\tilde{p}_G(\Omega)$ corresponds to the actual generation, p_G to the scheduled one and α is the vector of participation factor (contribution of each generator) [Vra+13b]. Related to the previous equation 6.8a, some papers [Roa16] or [CKA11] assume that each generator contributes according to its maximum nominal output, defining each α as:

$$\alpha_i = \frac{P_{G,i}^{max}}{\sum_{i \in G} P_{G,i}^{max}}, \forall i \in G \tag{6.9a}$$

Equation 6.9 attributes a specific participation factor according to the maximum capacity of each conventional generator over the total sum of their capacities. However, in this thesis, this value is assumed to be a variable to solve in the optimization problem, as it is assumed also in [Roa16]. As a result, in order to match the total power mismatch, it is vital to state that the sum of all the participation factors per time must be equal to unity:

$$\sum_{i \in G} \alpha_{i,t} = 1, \quad \forall t \tag{6.10a}$$

In consequence, the following set of equations represent the formulation for the CC-OPF:

$$\min_{\Theta} \sum_{t\in\mathcal{T}} \Big(\sum_{i\in\mathcal{C}} C_i^{\mathrm{E}}\ p_{i,t}^{DA} + \sum_{k\in\mathcal{K}} C_k^{\mathrm{G}}\ g_{k,t}^{DA} \Big) \tag{6.11a}$$

subject to

Day-Ahead constraints

$$0 \le p_{i,t}^{DA} \le P_i^{\max}, \forall i,t, \tag{6.11b}$$
$$0 \le w_{j,t}^{DA} \le W_{j,t}, \forall j,t, \tag{6.11c}$$
$$f_{n,r,t}^{DA} = B_{n,r}(\theta_{n,t}^{DA} - \theta_{r,t}^{DA}), \forall (n,r)\in\mathcal{L}, t \tag{6.11d}$$
$$-F_{n,r}^{\max} \le f_{n,r,t}^{DA} \le F_{n,r}^{\max}, \forall (n,r)\in\mathcal{L}, t \tag{6.11e}$$
$$-\pi \le \theta_{n,t}^{DA} \le \pi, \forall n,t,\ \ \theta_{n,t}^{DA} = 0, \forall n{:}\mathrm{ref}, t \tag{6.11f}$$
$$\sum_{i\in\mathcal{A}_n^I} p_{i,t}^{DA} + \sum_{j\in\mathcal{A}_n^J} w_{j,t}^{DA} - \sum_{(n,r)\in\mathcal{L}} f_{n,r,t}^{DA} = D_{n,t}^{\mathrm{E}}, \forall n,t, \tag{6.11g}$$
$$0 \le g_{k,t}^{DA} \le G_k^{\max}, \forall k,t, \tag{6.11h}$$
$$PR_m^{\min} \le pr_{m,t}^{DA} \le PR_m^{\max}, \forall m,t, \tag{6.11i}$$
$$pr_{u,t}^{DA} \le \Gamma_{m,u}\ pr_{m,t}^{DA}, \forall (m,u)\in\mathcal{Z}, t, \tag{6.11j}$$
$$q_{m,u,t}^{\mathrm{DA}^2} \le K_{m,u}^2 (pr_{m,t}^{\mathrm{DA}^2} - pr_{u,t}^{\mathrm{DA}^2}), \forall (m,u)\in\mathcal{Z}, t, \tag{6.11k}$$
$$0 \le q_{m,u,t}^{DA}, q_{m,u,t}^{\text{in DA}}, q_{m,u,t}^{\text{out DA}}, \forall (m,u)\in Z, t \tag{6.11l}$$
$$q_{m,u,t}^{DA} = \frac{q_{m,u,t}^{\text{in DA}} + q_{m,u,t}^{\text{out DA}}}{2}, \forall (m,u)\in\mathcal{Z}, t, \tag{6.11m}$$
$$h_{m,u,t}^{DA} = S_{m,u}\frac{pr_{m,t}^{DA} + pr_{u,t}^{DA}}{2}, \forall (m,u)\in\mathcal{Z}, t, \tag{6.11n}$$
$$h_{m,u,t}^{DA} = h_{m,u,(t-1)}^{DA} + q_{m,u,t}^{\text{in DA}} - q_{m,u,t}^{\text{out DA}}, \forall (m,u)\in\mathcal{Z}, t>1, \tag{6.11o}$$
$$h_{m,u,t}^{DA} = H_{m,u}^{0} + q_{m,u,t}^{\text{in DA}} - q_{m,u,t}^{\text{out DA}}, \forall (m,u)\in\mathcal{Z}, t=1, \tag{6.11p}$$
$$H_{m,u}^{0} \le h_{m,u,T}^{DA}, \forall (m,u)\in\mathcal{Z}, t=|\mathcal{T}| \tag{6.11q}$$
$$\sum_{k\in\mathcal{A}_m^K} g_{k,t}^{DA} - \sum_{i\in\mathcal{A}_m^G} \phi_i\ p_{i,t}^{DA} - \sum_{u:(m,u)\in\mathcal{Z}} (q_{m,u,t}^{\text{in DA}} - q_{u,m,t}^{\text{out DA}}) = D_{m,t}^{\mathrm{G}}, \forall m,t, \tag{6.11r}$$

Real-Time constraints

$$\mathbb{P}\Big[0 \le p_{i,t}^{DA} - \alpha_{i,t}\Omega \le P_i^{\max}\Big] \ge 1-\epsilon, \quad \forall i,t, \tag{6.12a}$$

$$f^{RT}_{n,r,t} = B_{n,r}(\theta^{RT}_{n,t} - \theta^{RT}_{r,t}), \forall (n,r) \in \mathcal{L}, t \tag{6.12b}$$

$$\mathbb{P}\Big[-F^{\max}_{n,r} \leq f^{RT}_{n,r,t} \leq F^{\max}_{n,r} \Big] \geq 1-\epsilon, \quad \forall (n,r) \in \mathcal{L}, t \tag{6.12c}$$

$$\mathbb{P}\Big[-\pi \leq \theta^{RT}_{n,t} \leq \pi \Big] \geq 1-\epsilon, \quad \forall n,t, \;\; \theta^{RT}_{n,t} = 0, \quad \forall n\text{:ref}, t \tag{6.12d}$$

$$\sum_{i \in I} \alpha_{i,t} = 1, \quad \forall t, \tag{6.12e}$$

$$\mathbb{P}\Big[0 \leq g^{DA}_{k,t} - \beta_{k,t}\Omega \leq G^{\max}_{k} \Big] \geq 1-\epsilon, \quad \forall k,t, \tag{6.12f}$$

$$\mathbb{P}\Big[PR^{\min}_{m} \leq pr^{RT}_{m,t} \leq PR^{\max}_{m} \Big] \geq 1-\epsilon, \quad \forall m,t, \tag{6.12g}$$

$$\mathbb{P}\Big[pr^{RT}_{u,t} \leq \Gamma_{m,u} \; pr^{RT}_{m,t} \Big] \geq 1-\epsilon, \quad \forall (m,u) \in \mathcal{Z}, t, \tag{6.12h}$$

$$q^{\mathrm{RT}^2}_{m,u,t} \leq K^2_{m,u}(pr^{\mathrm{RT}^2}_{m,t} - pr^{\mathrm{RT}^2}_{u,t}), \forall (m,u) \in \mathcal{Z}, t, \tag{6.12i}$$

$$q^{RT}_{m,u,t} = \frac{q^{\text{in RT}}_{m,u,t} + q^{\text{out RT}}_{m,u,t}}{2}, \forall (m,u) \in \mathcal{Z}, t, \tag{6.12j}$$

$$h^{RT}_{m,u,t} = S_{m,u}\frac{pr^{RT}_{m,t} + pr^{RT}_{u,t}}{2}, \forall (m,u) \in \mathcal{Z}, t, \tag{6.12k}$$

$$h^{RT}_{m,u,t} = h^{RT}_{m,u,(t-1)} + q^{\text{in RT}}_{m,u,t} - q^{\text{out RT}}_{m,u,t}, \forall (m,u) \in \mathcal{Z}, t > 1, \tag{6.12l}$$

$$h^{RT}_{m,u,t} = H^{0}_{m,u} + q^{\text{in RT}}_{m,u,t} - q^{\text{out RT}}_{m,u,t}, \forall (m,u) \in \mathcal{Z}, t = 1, \tag{6.12m}$$

$$\mathbb{P}\Big[H^{0}_{m,u} \leq h^{RT}_{m,u,T} \Big] \geq 1-\epsilon, \quad \forall (m,u) \in \mathcal{Z}, t = |\mathcal{T}| \tag{6.12n}$$

$$\sum_{k \in K} \beta_{k,t} = \sum_{i \in A^G} \alpha_{i,t}\phi_i, \quad \forall t \tag{6.12o}$$

$$0 \leq q^{RT}_{m,u,t}, q^{\text{in RT}}_{m,u,t}, q^{\text{out RT}}_{m,u,t}, \forall (m,u) \in Z, t \tag{6.12p}$$

where the set of optimization variables is
$\Theta = \{q^{DA}_{m,u,t}, q^{RT}_{m,u,t}, q^{\text{in DA}}_{m,u,t}, q^{\text{in RT}}_{m,u,t}, q^{\text{out DA}}_{m,u,t}, q^{\text{out RT}}_{m,u,t}, h^{DA}_{m,u,t}, h^{RT}_{m,u,t}, pr^{DA}_{m,t}, pr^{RT}_{m,t}, g^{DA}_{k,t}, p^{DA}_{i,t}, w^{DA}_{j,t}, \theta^{DA}_{n,t}, \theta^{RT}_{n,t}, \alpha_{i,t}, \beta_{k,t}, \}$.

Objective function 6.11a reflects the total cost after applying chance constraints. Due to the total power mismatch Ω, that follows a Gaussian distribution (μ'=0 and σ), the total expected costs through the time horizon is expected to be 0. As a result, only the first stage costs will be considered. Furthermore, all the constraints defining the first-stage (DA) remain precisely the same as in the other sections described in this thesis, as chance constraints are only applied in the recourse stage. However, in the recourse stage, all inequality constraints will be affected by the uncertainty factor. As a result, both capacity constraints (6.12a and 6.12f) for power and gas will modify their scheduled amount in DA depending on the participation factor and the

total power mismatch. In addition, $\alpha_{i,t}$ represents the participation factors of the power plants, which describes the contribution of each generator towards balancing the system in the recourse stage. The sum of all these elements must be equal to unity to ensure that any given fluctuation Ω is balanced. On the other hand, the $\beta_{k,t}$ corresponds to the participation factor of the gas suppliers that also ensures that all the gas sent to the GFPP in the recourse stage, will be balanced by the excess production of the gas supplier. Besides, both equations 6.12e and 6.12o assures that the power plants and gas suppliers produce the total power mismatch, meeting the demand for each period of time. Moreover, equation 6.12o assures that the gas supplier entirely supplies all the extra power produced in the GFPP in the recourse stage.
Chance constraints are also applied to the power flow as the amount of power sent or received changes depending on the mismatched amount. The Weymouth equation 6.12i will not be in CC form as it has been transformed previously into SOC form. Note that the Weymouth equation in its original form is an equality constraint. The same thing will happen to the non-negativity constraints, as the variables must be greater than 0. Finally, all the equations defining the pressures in the nodes will also be in CC form.

6.2.1 Solving method

Once the CC-OPF is formulated, it is essential to decide which of the two solving methods is more appropriate to use. There are two different approaches to solving such problems, approximation via samples or analytically with a known distribution.

6.2.1.1 Approximation via samples

This solving method tries to generate a large number of samples in order to know the probability distribution that the uncertainty factor follows. As a result, in order to know the number of samples needed, the following formula is used, following a lecture from DTU university [Ord18]:

$$N \geq \left\lceil \frac{1}{\epsilon} \frac{e}{e-1} \left(n_x - 1 + ln\left(\frac{1}{\psi}\right)\right)\right\rceil \tag{6.13a}$$

Where e is the Euler number, n_x is the number of decision variables and ψ corresponds to the level of confidence ensuring the solution to be in an ϵ-level solution.

Therefore, if it is considered that $\epsilon = 0.05$, $\psi = 0.0001$, the number of samples needed to solve the problem is:

$$N \geq \left\lceil 31.63\Big(n_x + 8.21\Big)\right\rceil \tag{6.14a}$$

As a result, in a problem with ten decision variables through a day (24 hours), the total number of samples needed raises to 7,851. Even in a situation with a few variables, the number of samples is high; therefore, solving by samples can be computationally hard. Thus, in this paper, it is assumed that the distribution of the forecast error is estimated by analyzing historical data.

6.2.1.2 Assuming known the probability distribution of wind power production

The co-optimization model can be transformed into an analytical form. The main reason why it has been chosen to use this approach is that it is computationally easier to solve compared to the sampling one, even though it can also be challenging to convert the chance constraints in an analytical form. As a result, the formulation in the previous section can be transformed as the following set of equations:

$$\min_{\Theta} \sum_{t\in\mathcal{T}} \Big(\sum_{i\in\mathcal{C}} C_i^{\mathrm{E}}\ p_{i,t}^{DA} + \sum_{k\in\mathcal{K}} C_k^{\mathrm{G}}\ g_{k,t}^{DA} \Big) + \mathbb{E}[Cost] \tag{6.15a}$$

subject to

Day-Ahead constraints

$$\textit{equations} \qquad 6.11b - 6.11r$$

Real-Time constraints

$$p_{i,t}^{DA} \leq P_i^{MAX} - \Phi_{\mathbb{P}}^{-1}(1-\epsilon)\big|\big|\alpha_{i,t}\sigma\big|\big|, \quad \forall i,t, \tag{6.15b}$$

$$p_{i,t}^{DA} \geq P_i^{MIN} + \Phi_{\mathbb{P}}^{-1}(1-\epsilon)\big|\big|\alpha_{i,t}\sigma\big|\big|, \quad \forall i,t, \tag{6.15c}$$

$$M_{n,r}\big(p_{i,t} + u_f - d\big) \leq F_{n,r}^{MAX} - \Phi_{\mathbb{P}}^{-1}(1-\epsilon)\Big|\Big|M_{n,r}(1-\alpha_i)\sigma\Big|\Big|, \quad \forall (n,r)\in\mathcal{L}, t \tag{6.15d}$$

$$M_{n,r}\big(p_{i,t} + u_f - d\big) \geq -F_{n,r}^{MAX} + \Phi_{\mathbb{P}}^{-1}(1-\epsilon)\Big|\Big|M_{n,r}(1-\alpha_i)\sigma\Big|\Big|, \quad \forall (n,r)\in\mathcal{L}, t \tag{6.15e}$$

$$\sum_{i \in I} \alpha_{i,t} = 1, \quad \forall t, \tag{6.15f}$$

$$g_{k,t}^{DA} \leq G_i^{MAX} - \Phi_{\mathbb{P}}^{-1}(1-\epsilon)\big|\big|\beta_{k,t}\sigma\big|\big|, \quad \forall k,t, \tag{6.15g}$$

$$g_{k,t}^{DA} \geq G^{MIN} + \Phi_{\mathbb{P}}^{-1}(1-\epsilon)\big|\big|\beta_{k,t}\sigma\big|\big|, \quad \forall k,t, \tag{6.15h}$$

$$PR_m^{\min} \leq pr_{m,t}^{RT} \leq PR_m^{\max}, \quad \forall m,t, \tag{6.15i}$$

$$pr_{u,t}^{RT} \leq \Gamma_{m,u}\ pr_{m,t}^{RT}, \quad \forall (m,u) \in \mathcal{Z}, t, \tag{6.15j}$$

$$q_{m,u,t}^{\mathrm{RT}^2} \leq K_{m,u}^2 (pr_{m,t}^{\mathrm{RT}^2} - pr_{u,t}^{\mathrm{RT}^2}), \forall (m,u) \in \mathcal{Z}, t, \tag{6.15k}$$

$$q_{m,u,t}^{RT} = \frac{q_{m,u,t}^{\text{in RT}} + q_{m,u,t}^{\text{out RT}}}{2}, \forall (m,u) \in \mathcal{Z}, t, \tag{6.15l}$$

$$h_{m,u,t}^{RT} = S_{m,u} \frac{pr_{m,t}^{RT} + pr_{u,t}^{RT}}{2}, \forall (m,u) \in \mathcal{Z}, t, \tag{6.15m}$$

$$h_{m,u,t}^{RT} = h_{m,u,(t-1)}^{RT} + q_{m,u,t}^{\text{in RT}} - q_{m,u,t}^{\text{out RT}}, \forall (m,u) \in \mathcal{Z}, t > 1, \tag{6.15n}$$

$$h_{m,u,t}^{RT} = H_{m,u}^{0} + q_{m,u,t}^{\text{in RT}} - q_{m,u,t}^{\text{out RT}}, \forall (m,u) \in \mathcal{Z}, t = 1, \tag{6.15o}$$

$$H_{m,u}^{0} \leq h_{m,u,T}^{RT}, \quad \forall (m,u) \in \mathcal{Z}, t = |\mathcal{T}| \tag{6.15p}$$

$$\sum_{k \in K} \beta_{k,t} = \sum_{i \in A^G} \alpha_{i,t}\phi_i, \quad \forall t \tag{6.15q}$$

$$0 \leq q_{m,u,t}^{RT}, q_{m,u,t}^{\text{in RT}}, q_{m,u,t}^{\text{out RT}}, \forall (m,u) \in Z, t \tag{6.15r}$$

where the set of optimization variables is
$\Theta = \{q_{m,u,t}^{DA}, q_{m,u,t}^{RT}, q_{m,u,t}^{\text{in DA}}, q_{m,u,t}^{\text{in RT}}, q_{m,u,t}^{\text{out DA}}, q_{m,u,t}^{\text{out RT}}, h_{m,u,t}^{DA}, h_{m,u,t}^{RT}, pr_{m,t}^{DA}, pr_{m,t}^{RT}, g_{k,t}^{DA}, p_{i,t}^{DA}, w_{j,t}^{DA}, \theta_{n,t}^{DA}, \alpha_{i,t}, \beta_{k,t}, \}$.

In CC-OPF, when assuming known the probability distribution of the wind power production, constraint 6.12a is transformed into two new equations, limiting the maximum and minimum amount to produce (equations 6.15b and 6.15c). Constraint 6.15b states that the production in the first stage of each generator must be lower or equal than its maximum capacity minus the random fluctuation of the total power mismatch. The $\Phi_{\mathbb{P}}^{-1}(1-\epsilon)$ is considered as the inverse of the cumulative distribution function of the known probability distribution [Roa16] (in this case, Gaussian), evaluated in a specific risk factor (ϵ) and multiplied by the norm of the participation factor and the standard deviation. On the other hand, equation 6.15c limits the minimum quantity to be produced in the recourse stage. On the left-hand side of equation 6.15d and 6.15e, a new term appears (M) corresponding to the matrix of Power Transfer Distribution Factor (PTDF), relating the line flows to the power injections. This matrix is defined as:

$$M = B_F \begin{bmatrix} \left(\tilde{B}_{Bus}\right)^{-1} & 0 \\ 0 & 0 \end{bmatrix}$$

Where B_F represents the line susceptance and $\tilde{B}_{Bus}$ is the bus susceptance [Vra+13a]. Although all terms are represented as matrices, in the set of equations presented, the term $M_{n,r}$ is considered as a parameter obtained from the matrix M. As a result, the obtained amount to flow (according to the linear DC approximation [WWS13]) or to receive (depending on the sign of the left-hand side expression) plus the uncertainty term must not exceed the maximum capacity of the transmission line. The second term of the right-hand side of the equations relates to the power transfer distribution factor with the participation factor of all generators located in a different node than the starting one (n). Moreover, it also multiplies both terms with the standard deviation and the inverse of the probability distribution factor of the wind fluctuation. On the other hand, equation 6.15e represents the same constraint but allowing that the power flow from node n to node r can be the other direction (from r to n).
Equation 6.15f states that the summation of all the participation factors of the power generators must be equal to unity. This constraint, therefore, assures that the power generators supply all the variation in power production in the recourse stage.
On the other hand, focusing on the gas system, equations 6.15g and 6.15h limits the maximum amount to produce in the recourse stage. Although this maximum amount can indeed be exceeded with a probability of ϵ. The amount produced in the first stage must be lower than the maximum capacity minus the inverse of the known probability distribution evaluated in a specific risk factor. Besides, all this term is multiplied by the norm of the gas participation factor and the standard deviation of the total power mismatch. Equation 6.15h limits the minimum amount of natural gas to supply in the recourse stage.
Referring to the inequalities relating the pressure at each node (6.15i and 6.15j), the assumption of not applying chance constraints has been considered. There were some limitations in terms of relating both terms, the pressure in the nodes and the uncertainty value of the renewables. The unit of the pressure is in [psig], and the uncertain value is quantified by the power production in [MWh]. As a result, the lack of having a parameter relating pressure with power units has led to skipping the development of its chance constraint form.
The Weymouth equation shown in constraint 6.15k is already relaxed into its second-order cone (SOC); therefore, applying CC is not needed. Besides, the following set

of equations (6.15l - 6.15o) are equalities. In consequence, chance constraints do not apply to them.
Similarly to 6.15i and 6.15j, inequality 6.15p that shows the minimum amount of linepack to be in the pipeline at the end of the time horizon to avoid depletion, is not converted into its CC form. It occurs the same as with the pressure constraints, due to the lack of a factor relating the amount of linepack with the uncertainty sources. Therefore, it is also assumed not to transform the constraint into its CC form. When it comes to the gas coupling constraint, equation 6.15q computes that the total amount produced by the GFPP (reflected with the participation factors) in the recursive stage must equal the participation factor of the gas suppliers. It is important to highlight that, in case of the gas system, the participation factor can be greater than 1, unlike the power system.

CHAPTER 7

Description of the small scale system

This section contains a description of the base case applied in this master thesis. It is essential to highlight that the mathematical formulation presented in this paper is not based on this specific base case. On the contrary, it is this base case the one used to understand and analyze the results obtained from the generic mathematical formulation.

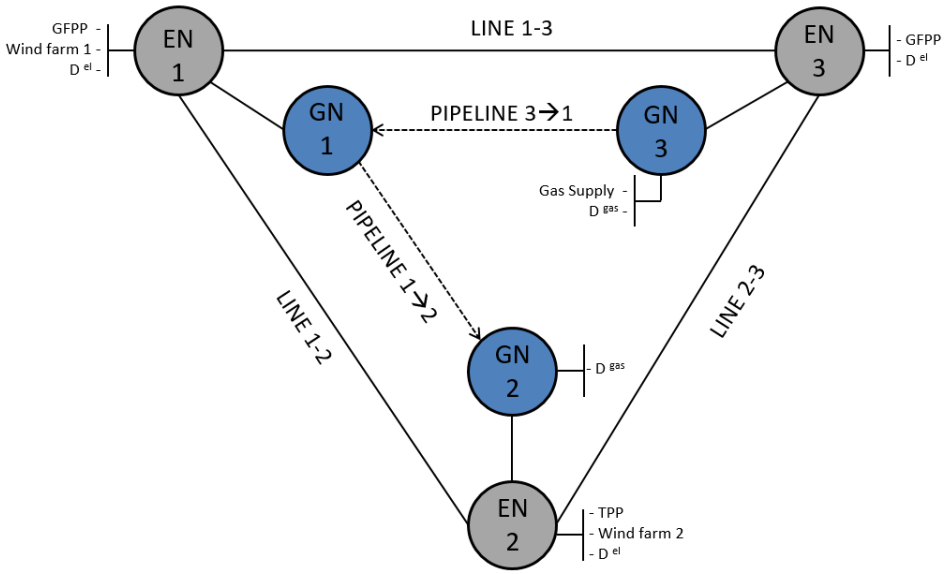

Figure 7.1: Small scale system.

Figure 7.1 illustrates a 3-node network formed by three different electricity and gas nodes with interconnections between them. For this specific case study, a distinction is made between power and gas nodes. As a result, the power nodes (shown in figure 7.1 as *EN*) are i1, i2 and i3 whereas the natural gas nodes (*GN*) are called k1, k2 and k3 located in nodes 1, 2 and 3, respectively. Power flows between the three nodes (i1, i2, i3) in any desired direction according to their needs in every time period. In order to do that, transmission lines are used with different characteristics depending on the connected nodes (continuous lines shown in Figure 7.1). On the other hand, natural gas can only flow from k3 to k1 and from k1 to k2. The gas flow between k2 and k3 is not available; therefore, anything sent to k2 will have to be sent first to k1. In this case, pipelines (discontinuous lines) will be in charge to flow the natural gas from one place to another, and each of them will contain certain characteristics to perform it.

Node i1 contains a gas-fired power plant with a maximum capacity of $P^{max} = 152$ [MW] with a conversion factor of $\phi_1 = 12.65$ [kcf/MWh], a wind farm with $P^{max} = 500$ [MW] and a share of $\frac{1}{3}$ of the total electricity demand. Node k1 has no gas demand. Furthermore, node i2 contains a thermal power plant with a maximum capacity of $P^{max} = 400$ [MW] and an electricity cost of $cost_{elec} = 44.55$ [$/MW], another wind farm with $P^{max} = 1000$ [MW] and a share of $\frac{1}{3}$ of the total electricity demand. On the other hand, the natural gas node k2 only possess a share of 0.9 of the total natural gas demand, without having any gas supply. Finally, node k3 has a large natural gas supply of 15,000 [kcf] with a cost of $cost_{NG} = 2.8$ [$/kcf] and a share of 0.1 of the total gas demand, whereas the electricity node i3 has another gas-fired power plant with $P^{max} = 155$ [MW] with a conversion factor of $\phi_3 = 14.88$ [kcf/MWh], no wind farms and an electricity gas demand with a share of $\frac{1}{3}$ of the total electricity demand. As also evident in Figure 7.1, node i3 can exchange power with the two other nodes, but node k3 can uniquely send natural gas to k1. Moreover, k3 will be responsible for supplying gas to the rest of the nodes in order to meet the demand as it is the only one capable of obtaining this commodity.

The following tables (appendix tables B.1, B.2 and B.3) summarizes the data explained previously and contain all the input values introduced in the optimization problem to solve the proposed case.

CHAPTER 8

Results

This chapter will contain the results of all the formulation explained in the previous sections applied to a specific small scale system (chapter 7). Moreover, all the results obtained from the different approaches applied will afterwards be compared and constrasted to understand, in a better way, the numbers obtained.

8.1 Unidirectional deterministic implementation (UDI)

8.1.1 One stage programming without linepack

As mentioned previously, this subsection refers to the results obtained when there is no natural gas storage in the pipelines. As a result, in the mathematical formulation, all the constraints related to the linepack in each of the pipelines per time steps are not considered. Furthermore, a new constraint is added in order to enforce that the introduced amount in a certain node will exit in its adjacent one.

$$q^{\text{in}}_{m,u,t} = q^{\text{out}}_{m,u,t}, \forall (m,u), t \in \mathcal{Z}, T \tag{8.1a}$$

Moreover, as a second-order cone relaxation has been imposed in the formulation, it is necessary to check the values obtained and its tightness in the Weymouth equation (constraint 5.1k) as in reality, the Weymouth equation needs to be fulfilled. It is important to remember that the SOC relaxation is only a tool to be able to solve problems with quadratic equality constraints. In optimal conditions, the constraint obtained by SOC needs to behave as equality. As a result, the following error formula has been applied:

$$Error = \frac{\sqrt{\sum_{(m,u)}^{\mathcal{Z}} \sum_{t}^{T} (\frac{b_{m,u,t} - a_{m,u,t}}{b_{m,u,t}})^2}}{|Z||T|} \tag{8.2a}$$

where:

$$b_{m,u,t} = K^2_{m,u}(pr^2_{m,t} - pr^2_{u,t}) \quad \forall(m,u), t \in \mathcal{Z}, T \tag{8.3a}$$

$$a_{m,u,t} = q^2_{m,u,t} \quad \forall(m,u), t \in \mathcal{Z}, T \tag{8.3b}$$

$|Z|$ and $|T|$ are the total amount of pipelines and time steps through the horizon, respectively. The error is calculated as the square root of the sum of the squared relative errors per pipeline and time step. Afterwards, the result is divided by the total amount of pipelines and time horizon, to obtain an average. Furthermore, a frequency plot will also be included to analyze the relative error obtained in each of the pipelines for every time step in order to extract conclusions together with the previous error equation 8.2a.

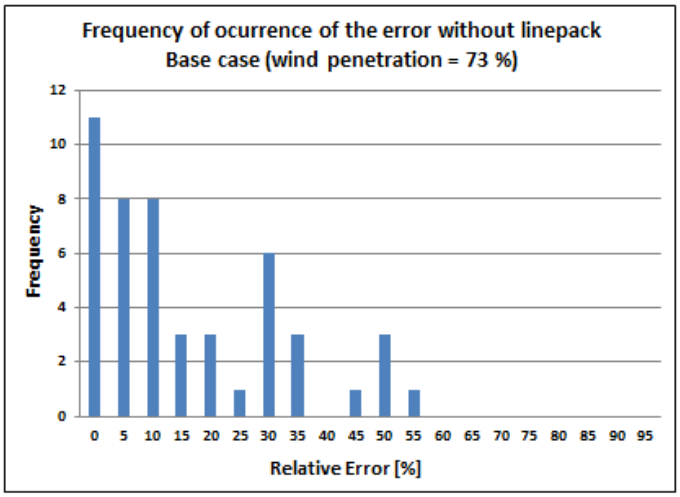

Figure 8.1: frequency of relative error percentage without linepack in base case.

$$Relative\ error = \frac{b_{m,u,t} - a_{m,u,t}}{b_{m,u,t}} \quad \forall(m,u), t \in \mathcal{Z}, T \tag{8.4a}$$

Figure 8.1 illustrates the frequency of error through time and pipelines with a wind penetration of approximately 73 %, resulting a total amount of 48 solutions to check (2 pipelines through a day). The 0 value in the *error* axis corresponds to the amount of times in which equation 8.2 results in 0. The other values correspond to an interval formed by each of the value in the graph and its previous one. For example, eight times the relative error has been between 0 (not included) and 5 (included). Figure

8.1 shows that 11 times out of 48, the relative error corresponds to 0 and 16 times the relative error results in between 0 and 10 %. The total error obtained is 3.03 %.

The total system costs raise to $6.89 \cdot 10^5$ \$. Later on, these values will be compared and contrasted with the results obtained with linepack, in order to have an idea of how linepack can benefit the coupled system. However, it is vital to bear in mind the second-order cone relaxation applied to the Weymouth equation. It means that in reality, the constraint behaves as an equation (not inequation) so both sides of the constraint need to coincide. As a result, it might be possible that if the tightness of the relaxation was higher, it could indeed raise the total system costs.
On the other hand, as mentioned previously, results vary according to the inputs introduced. In the following example, it has been changed the natural gas flow constant of the pipeline connecting node 1 and 2, from 28 to 24 ($K_{1,2} = 24$). Moreover, the compressor factor of both pipelines will also be modified ($\Gamma_{1,2} = 1.4$ and $\Gamma_{3,1} = 1.8$). Finally, the minimum pressure in all the natural gas nodes will be 50 [psig]. However, the values of the maximum pressure will vary according to each natural gas node (350 [psig] for both gas nodes 1 and 2 and 450 [psig] for gas node 3. The following table summarizes all the modifications made in comparison to the base case:

INPUT DATA				
Pipeline information				
	Base case		Case 1	
	Pipeline 1-2	Pipeline 3-1	Pipeline 1-2	Pipeline 3-1
$K_{m,u}$	28	28	24	28
$\Gamma_{m,u}$	1.1	1	1.4	1.8
Natural gas nodes information				
Natural gas nodes	Base case		Case 1	
	Min pressure [psig]	Max pressure [psig]	Min pressure [psig]	Max pressure [psig]
1	100	500	50	350
2	100	500	50	350
3	100	500	50	450

Table 8.1: Modifications applied in respect of the base case input data.

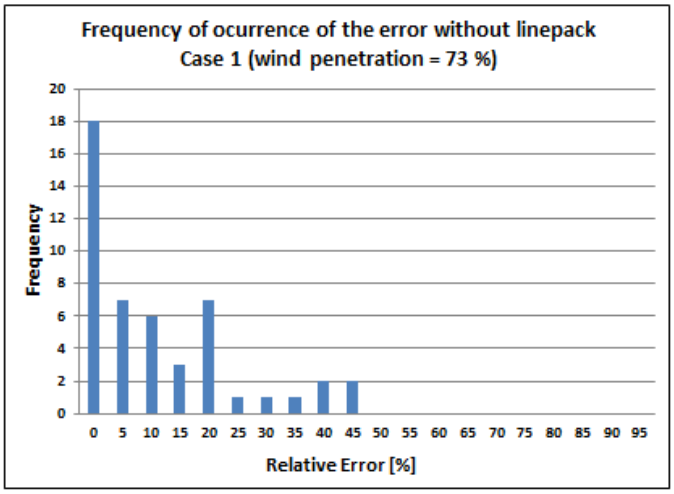

Figure 8.2: Frequency of relative error percentage without linepack in case 1.

By applying all the modifications shown in table 8.1, Figure 8.2 illustrates the obtained frequency plot. It reflects the frequency of the relative errors per pipeline and time steps. It shows that 18 times out of 48, the relative error has laid on 0 %, seven more times than in the base case example. Moreover, the maximum relative error relies on 45 %, 10 % less than in the base case. Apart from this, the total error obtained by applying equation 8.2 results in 2.24 %, reducing the total obtained error from the base case in 0.79 %. With a lower error, this graph reflects how the difference between both sides of the Weymouth equation reduces and thus, its cost will be affected. As a result, the total cost increases to $6.94 \cdot 10^5$ \$. This happens because as the tightness between the sides in the Weymouth equation increases, the squared flow of natural gas in the pipeline will be more similar to the right side value, leading to a possible increment in the total costs.

8.1.2 One stage programming with linepack

This subsection will contain all the results discussed in the previous one but taking into consideration the effect of the natural gas storage. As a result, the set of equations used in this case are the same as the ones described in subsection 3.3 (equation 8.1 is not considered, as with natural storage, it does not have to be fulfilled). The equations used to calculate the errors are the same ones as described in both equations 8.2 and

8.4. To start with, a frequency plot of the relative errors with linepack will be added to observe where the most frequent errors lay and which ones are rarer:

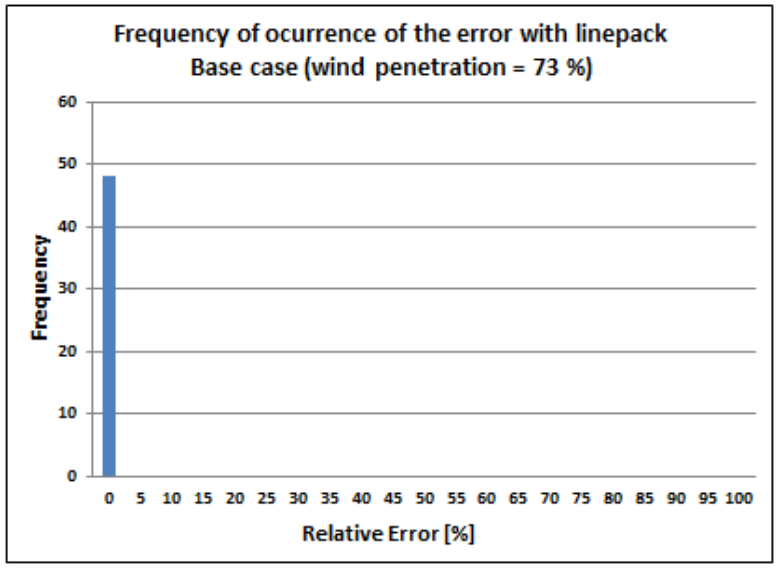

Figure 8.3: Frequency of relative error percentage with linepack.

Figure 8.3 illustrates that with natural gas storage, all the relative errors correspond to a value of 0. This means that by the addition of linepack, the system behaves in a way that fully fulfils the Weymouth equation. The system is completely tight, and the results are fully reliable. The total error (according to equation 8.2) corresponds to $2.24 \cdot 10^{-7}\%$ therefore, the system behaves accomplishing the initial Weymount equation (constraint 5.1k). Below, both tables 8.2 and 8.3 reflect its tightness numerically in every time step per pipeline:

CONVERGENCE CHECK FOR PIPELINE CONNECTING GAS NODE 1 WITH 2				
time period	q_{12}	q_{12}^2	$K_{12}^2(pr_1^2 - pr_2^2)$	**Relative Error**
t1	5090.99	25918168.26	25918169.97	$6.59 \cdot 10^{-6}$ %
t2	6667.41	44454380.89	44454381.99	$2.48 \cdot 10^{-6}$ %
t3	6988.17	48834457.39	48834458.31	$1.89 \cdot 10^{-6}$ %
t4	6599.87	43558232.32	43558232.83	$1.17 \cdot 10^{-6}$ %
t5	6816.32	46462226.25	46462226.68	$9.29 \cdot 10^{-7}$ %
t6	6760.60	45705756.65	45705757.09	$9.45 \cdot 10^{-7}$ %
t7	7143.49	51029392.45	51029392.90	$8.86 \cdot 10^{-7}$ %
t8	6714.87	45089467.53	45089469.14	$3.58 \cdot 10^{-6}$ %
t9	7066.60	49936803.83	49936807.25	$6.83 \cdot 10^{-6}$ %
t10	7725.79	59687855.24	59687856.17	$1.55 \cdot 10^{-6}$ %
t11	7562.60	57192944.18	57192944.79	$1.07 \cdot 10^{-6}$ %
t12	7765.85	60308464.32	60308465.23	$1.51 \cdot 10^{-6}$ %
t13	7389.88	54610301.62	54610302.32	$1.28 \cdot 10^{-6}$ %
t14	7775.99	60466008.67	60466009.19	$8.56 \cdot 10^{-7}$ %
t15	7404.75	54830284.05	54830284.42	$6.84 \cdot 10^{-7}$ %
t16	7787.47	60644638.69	60644639.00	$5.22 \cdot 10^{-7}$ %
t17	7894.42	62321804.70	62321804.78	$1.32 \cdot 10^{-7}$ %
t18	7597.84	57727244.78	57727244.90	$2.14 \cdot 10^{-7}$ %
t19	7618.75	58045393.88	58045393.99	$1.81 \cdot 10^{-7}$ %
t20	7770.82	60385677.10	60385677.20	$1.62 \cdot 10^{-7}$ %
t21	7371.74	54342563.88	54342564.23	$6.45 \cdot 10^{-7}$ %
t22	7421.43	55077667.86	55077668.02	$2.89 \cdot 10^{-7}$ %
t23	6089.67	37084043.34	37084043.36	$5.79 \cdot 10^{-8}$ %
t24	4849.69	23519462.54	23519462.55	$4.95 \cdot 10^{-7}$ %

Table 8.2: Convergence check of natural gas flow from natural gas node 1 to 2.

CONVERGENCE CHECK FOR PIPELINE CONNECTING GAS NODE 3 WITH 1				
time period	q_{31}	q_{31}^2	$K_{31}^2 \cdot (pr_3^2 - pr_1^2)$	**Relative Error**
t1	9090.99	82646075.38	82646077.58	$2.67 \cdot 10^{-6}$ %
t2	9706.98	94225444.40	94225444.82	$4.39 \cdot 10^{-7}$ %
t3	9031.68	81571314.42	81571314.65	$2.90 \cdot 10^{-7}$ %
t4	8832.03	78004740.22	78004740.53	$3.97 \cdot 10^{-7}$ %
t5	8271.81	68422814.77	68422814.93	$2.35 \cdot 10^{-7}$ %
t6	7870.51	61944873.60	61944873.76	$2.56 \cdot 10^{-7}$ %
t7	7574.32	57370391.32	57370391.69	$6.30 \cdot 10^{-7}$ %
t8	7974.55	63593392.44	63593392.63	$2.94 \cdot 10^{-7}$ %
t9	8173.19	66800961.22	66800961.34	$1.82 \cdot 10^{-7}$ %
t10	7888.56	62229453.62	62229453.66	$6.44 \cdot 10^{-8}$ %
t11	8129.39	66087010.81	66087010.87	$9.14 \cdot 10^{-8}$ %
t12	7978.68	63659282.63	63659282.73	$1.50 \cdot 10^{-7}$ %
t13	8346.69	69667214.80	69667215.20	$5.77 \cdot 10^{-7}$ %
t14	8098.35	65583322.27	65583322.64	$5.71 \cdot 10^{-7}$ %
t15	8378.80	70204364.19	70204364.26	$1.08 \cdot 10^{-7}$ %
t16	8126.52	66040353.99	66040354.06	$1.09 \cdot 10^{-7}$ %
t17	8178.52	66888167.83	66888167.90	$1.15 \cdot 10^{-7}$ %
t18	8597.97	73925096.21	73925096.28	$9.84 \cdot 10^{-8}$ %
t19	8821.93	77826468.57	77826468.62	$6.22 \cdot 10^{-8}$ %
t20	8772.14	76950406.35	76950406.41	$8.15 \cdot 10^{-8}$ %
t21	8995.57	80920294.30	80920294.52	$2.76 \cdot 10^{-7}$ %
t22	8647.74	74783486.70	74783486.75	$8.67 \cdot 10^{-8}$ %
t23	4081.07	16655107.33	16655107.38	$2.76 \cdot 10^{-7}$ %
t24	2796.09	7818101.65	7818101.67	$2.43 \cdot 10^{-7}$ %

Table 8.3: Convergence check of natural gas flow from natural gas node 3 to 1.

Both tables 8.2 and 8.3 illustrate appropriate values with a convergence check of almost 0. In addition, the objective value raises to $7.02 \cdot 10^5$ \$.

On the other hand, in order to understand the role of the linepack and the flexibility that adds in an integrated system, the natural gas flow between the k1 and k2 nodes for each period of time is shown in the following table 8.4. It has been chosen to show the results between these two nodes since they can not obtain their own natural gas and, as a result, everything flows from k3. Thus, the effect of the linepack between these two nodes is more noticeable than the existing one between k3 and k1.

LINEPACK IN PIPELINE FROM NODE 2 TO 1				
time period	q_{in1}	q_{out2}	$h_{pipeline12}$	**Natural Gas Demand k2**
t1	3881.98	6300	36881.98	6300
t2	7304.82	6030	38156.80	6030
t3	8216.33	5760	40613.13	5760
t4	7349.73	5850	42112.86	5850
t5	7692.64	5940	43865.51	5940
t6	7491.21	6030	45326.71	6030
t7	7311.97	6975	45663.68	6975
t8	6409.74	7020	45053.42	7020
t9	6438.20	7695	43796.62	7695
t10	7621.58	7830	43588.20	7830
t11	7295.20	7830	43053.40	7830
t12	7836.70	7695	43195.11	7695
t13	7084.76	7695	42584.87	7695
t14	7856.98	7695	42746.84	7695
t15	7249.49	7560	42436.34	7560
t16	7879.93	7695	42621.27	7695
t17	7688.83	8100	42210.11	8100
t18	7095.69	8100	41205.79	8100
t19	7137.51	8100	40243.30	8100
t20	7711.64	7830	40124.94	7830
t21	7318.48	7425	40018.43	7425
t22	8092.87	6750	41361.29	6750
t23	6239.33	5940	41660.63	5940
t24	3669.37	6030	39300.00	6030

Table 8.4: Convergence check of natural gas flow from natural gas node 3 to 1.

With an initial $H_0 = 39300$ [kcf], table 8.4 illustrates how useful can linepack be for natural gas storage. The excess of gas flown inside the pipeline is stored for future usage. This means that all the extra production obtained from the natural gas supply is not lost. Moreover, even if in this specific case it does not occur, linepack can be significantly beneficial for those periods of time with a peak demand, higher than the maximum capacity, as the extra amount needed can be provided by the natural gas stored in the pipelines. Furthermore, in case of variability in the natural gas price, it can be potentially beneficial in order to reduce the total expenses as the extra production obtained during periods of low cost can be stored and used in future more expensive periods. By the end of the time horizon, t = t24, the minimum linepack in

the pipeline must be equal or greater than H_0.

Furthermore, the following plot represents the total behaviour of linepack in the base case (taking into consideration the linepack in both pipelines):

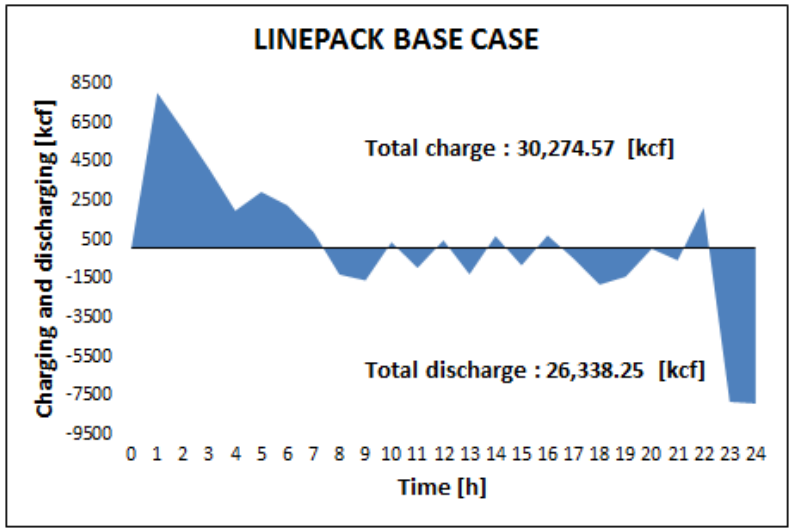

Figure 8.4: Profile of the charge and discharge of natural gas in both pipelines.

Both figure 8.4 and table 8.4 show how linepack adds flexibility in our system. However, focusing on the total linepack, figure 8.4 shows how there is a peak charge in the firsts time steps that will afterwards be used to fulfil the demand. After more or less the seventh hour, the profile changes basically into discharge (with small charges in certain hours) until the last 2 hours, where it consumes large quantities of natural gas but always respecting constraint 5.2q.

It is essential to highlight that even the pipelines may start with an initial amount of natural gas stored (in this specific problem), gas suppliers need to ”refill” the pipelines with gas in order to charge them with a sufficient amount by the end of the period T. This is done in order to avoid depletion.

8.1.3 Study cases

After analyzing linepack's behaviour in the base case example, it is interesting to understand how linepack can vary its profile depending on the specific situation encountered, as the base case is an invented example. As a result, this section focuses on the impact of linepack in the system and how dependent it can be in respect of some of the introduced parameters. Wind variability and gas demand are the chosen inputs that will be modified for further study. The reason why wind variability is considered for the specific analysis is that it is interesting to observe the variations in the linepack depending on the wind profiles. Moreover, as in the studied case, there is only one natural gas supplier, increasing or decreasing the natural gas demand will be relevant to check the linepack of the entire system and understand the numbers obtained in the base case.

8.1.3.1 Wind variability

Previous results in this paper have shown how linepack can support the power system to produce electricity in case of need. Renewables are indeed a source of uncertainty, and it is difficult enough to predict the model of the incoming wind. In the studied base case, it is assumed that the incoming wind follows a descending wind profile with its highest income in the very beginning of the day and lowest, on the other hand, at the end of the day with some fluctuations in between. The following image represents the wind profile of the base case:

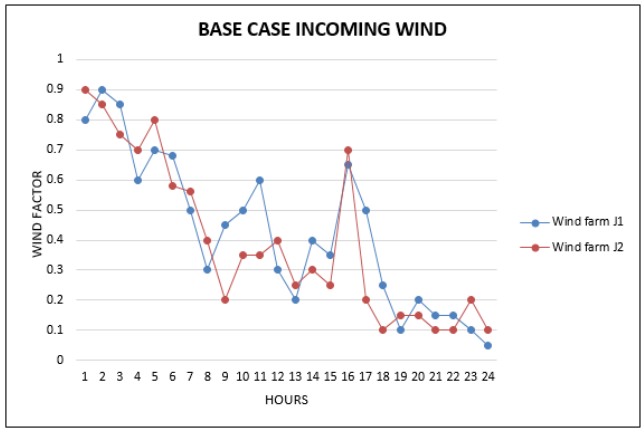

Figure 8.5: Profile of incoming wind in the base case example.

As a result, it is interesting to observe possible changes in the system when the incoming wind has considerably different profiles. Hence, the following graphs show the proposed wind incomes to study with their linepack profiles:

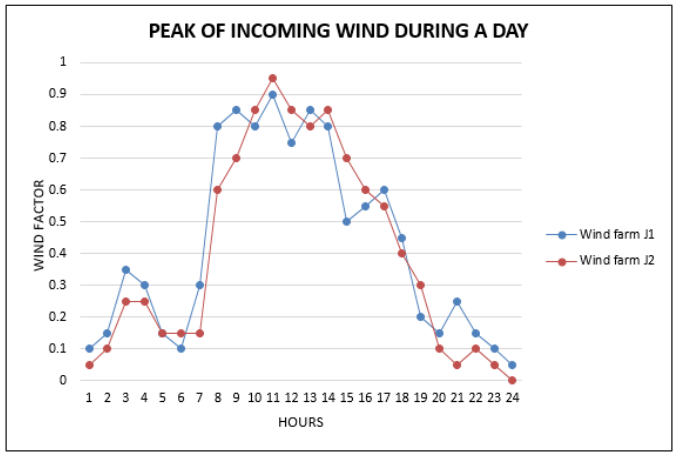

Figure 8.6: Profile of incoming wind with one peak.

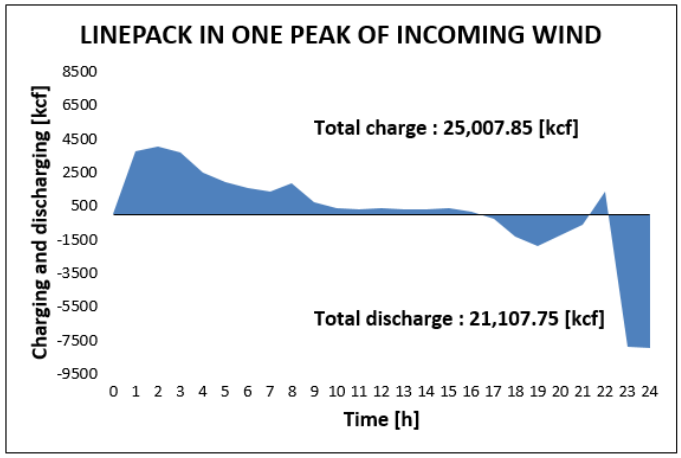

Figure 8.7: Profile of the charge and discharge of natural gas in both pipelines.

Figure 8.7 illustrates the linepack profile of the incoming wind shown in figure 8.6. It reflects how the profile is charging natural gas in the pipelines at each period of time in order to be able to supply the demand afterwards. As the incoming wind is

not that high during the first third of the day, figure 8.7 illustrates how the amount of natural gas charged in the pipelines results in a lower quantity compared to the base case. This is because the low wind income forces the gas supplier to send natural gas to the GFPP so that they can produce electricity at a lower price, in comparison to the thermal power plants. At around the second third of the day, due to the high income of wind, the linepack profile shows how it is still charging small quantities of gas until the 16th hour. This happens because the wind power production can supply the demand fully. Thus, the gas supplier does not need to send natural gas to the GFPP for electricity production. From that time, the incoming wind also decreases provoking the system to use natural gas from the pipelines. Besides, due to the small peak during the 21-22 hour, more wind is used to obtain power and, as a result, the pipelines recharge a small amount of natural gas. Finally, by the end of the day, when there is no wind, large amounts of natural gas are used to supply both gas and power demands.

On the other hand, the following figures will show another new situation with the incoming wind with two peaks in a day and its linepack profile:

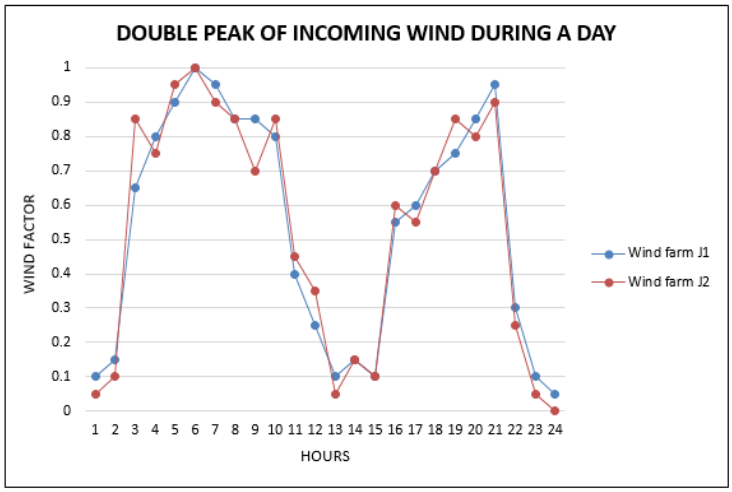

Figure 8.8: Profile of incoming wind with two peaks.

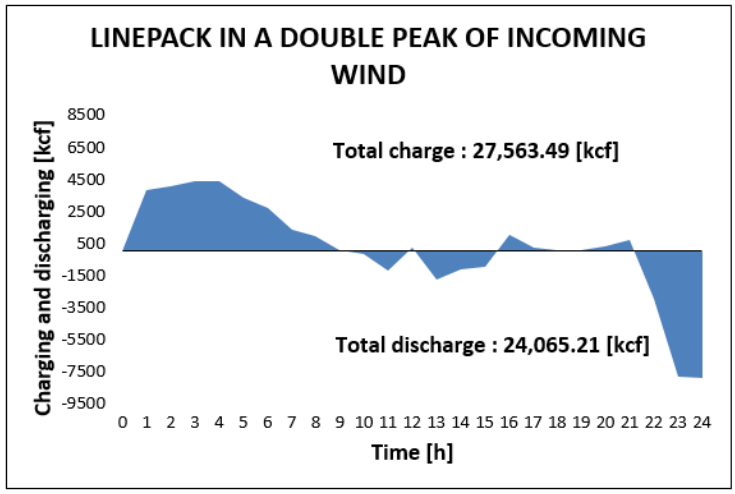

Figure 8.9: Profile of the charge and discharge of natural gas in both pipelines..

Similarly to the other two examples (base case and one peak of incoming wind), the linepack profile exhibit a period of charging natural gas in the pipelines for the first 8 hours. However, it is when the incoming wind starts to decrease when the system takes advantage of the charged amount of linepack and uses it to supply either the natural gas or the power demand, depending on the hour. What is certain is that the system will need natural gas to produce electricity from the 13th to the 15th hour of the day. Moreover, as the wind income starts to increase from the 16th until the 21st hour, the linepack profile illustrates it charges the pipelines from natural gas. Finally and coinciding with the other two examples, a large amount of natural gas is used to supply both power and natural gas demands as, by the end of the day, figure 8.8 shows barely incoming wind.

To conclude, these three explained examples represent invented situations in order to demonstrate how the linepack in the pipelines can modify its profile in order to benefit the most to the entire system. It is essential to highlight the fact that all three examples charge their pipelines at the beginning of the day. This occurs because the total natural gas capacity is large enough to supply the total demand and still charge the pipelines. As a result, the only difference between the three examples will be the quantity of natural gas stored, depending on the incoming wind in each situation. Equivalently, all three examples finish the day with basically no wind. Thus, all three have the same ending linepack profile. Large amounts of gas will be discharged at the

end of the day in order to make the most profit of it and also respecting the minimum amount in order to avoid depletion. Also, no total system costs are compared as with different profiles of incoming wind, different amounts of wind penetration each of the examples will obtain.

8.1.3.2 Gas demand

Another interesting factor to analyze is the gas demand and the behaviour of the entire system according to its fluctuations. As a result, by having just one gas supplier in the base case, it is proposed to vary the gas demand of the total system in ± 15 %, study the linepack´s behaviour and how sensitive it can be due to variations in the gas demand. The following figures illustrate the linepack´s behaviour of the entire system when the gas demand experiences ± 15 %:

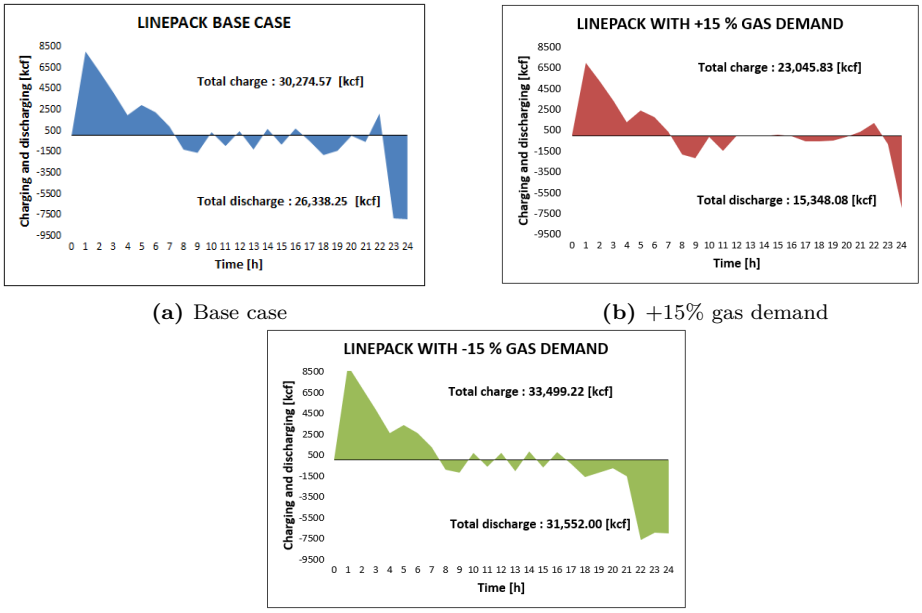

(a) Base case

(b) +15% gas demand

(c) -15 % gas demand

Figure 8.10: Linepack charge/discharge with different gas demands.

Figure 8.10 illustrates a comparison of the linepack's profile of the entire system depending on the gas demand. By increasing the total gas demand in 15 %, it implies that less natural gas is used for linepack's purposes as more quantity needs to be supplied in order to fulfil the gas demand. As a result, the total amount charged/discharged of natural gas in the pipelines will result lower than in the other two cases.
All three profiles illustrate the similarities with each other.The same profile is described until the tenth hour, experiencing a peak charge in the first hour with a steep descend until the 4th hour of the day. Note that this descend does not mean discharging but merely a reduced amount of natural gas is charged in the pipeline. Moreover, figure 8.10b reflects that after discharging natural gas from the 7th hour of the day until the 11th (except the 10th hour, where it does not occur anything) there is no linepack activity and the system does not charge or discharge until the 16th hour. After that, the system experiences a minor discharge for three hours and low peak charge before a large quantity of natural gas is used for the last two hours of the day. On the other hand, the other two illustrations 8.10a and 8.10c show a similar profile throughout the entire time horizon. Almost the same fluctuations occur from the 10th hour until the 16th. However, image 8.10c shows a copious discharge of natural gas in the system, more significant than the other two cases. This is because even if the three figures illustrate the same profile for specific hours, the quantities differ as with less gas demand and a higher amount can be used to charge the pipelines for further use.

8.2 Two stage programming with linepack

8.2.1 Solution Check

Similarly to the one-stage programming results, this section will first focus on the convergence check of the Weymouth equation for both DA and RT stages (or first and recourse stage, respectively). However, it is vital to bear in mind the existence of 2 stages; therefore, both stages need to be checked. The error formula explained in section 8.1 (equation 8.2) is also used in this chapter to check how tight the Weymouth equation is after applying the SOC relaxation in both stages.
For the application of this two-stage programming into the small scale system, it has been considered the potential of incoming wind in the recourse stage of 99% of the amount forecasted (per windfarm and time step) in the first stage. As a result, the

following graph will contain the frequency of relative error percentage obtained in the first stage:

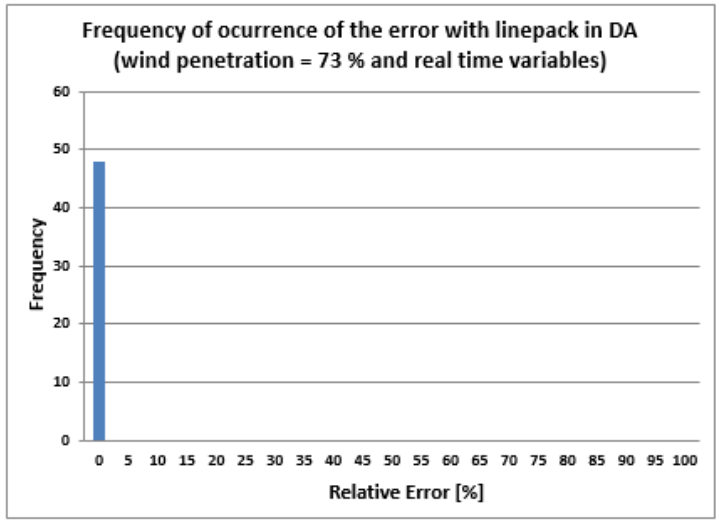

Figure 8.11: Frequency of relative error percentage with linepack in the 1st stage (DA).

Figure 8.11 illustrates the frequency of the relative error of the base case study considering two pipelines and uniquely the DA stage. Equation 8.4 is also being used in order to compute in which range the relative error is located. As a result, the same graph is obtained compared to the UDI with linepack. By computing the error using the formula shown in 8.2, and obtaining a wind penetration of 73%, a total error of $1.44 \cdot 10^{-5}\%$ is obtained, validating the obtained results.
On the other hand, as it is two-stage programming, it is also essential to check the accomplishment of the Weymouth equation in the recourse stage to validate the model. Hence, the following graph will also show the relative error of the real-time stage:

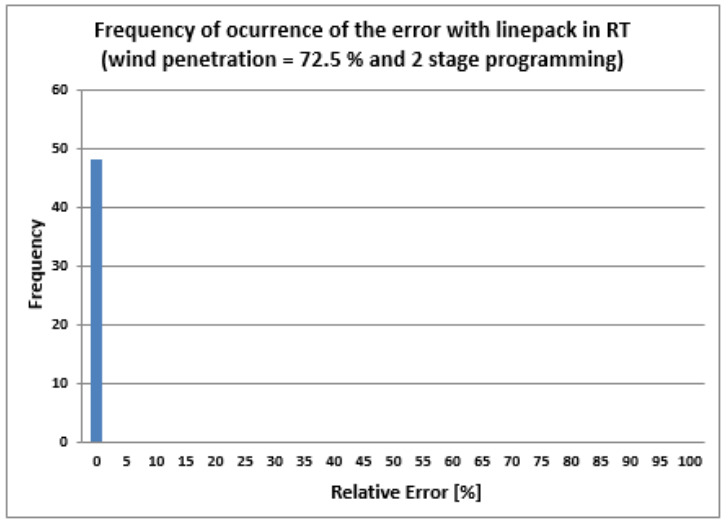

Figure 8.12: Frequency of relative error percentage with linepack in the 2nd stage (RT).

Figure 8.12 also shows how all the relative errors of the variables obtained in the recourse stage relies on 0. These values ultimately validate the two-stage model, allowing to continue analyzing the results thoroughly. Moreover, the total error obtained in this real-time stage raises to $1.44 \cdot 10^{-5}\%$, the same as the value obtained in the day ahead stage. Due to the assumption of obtaining a potential of 99 % of incoming wind (from the forecasted values in the first stage), the total wind penetration is 72.5%, 0.5 % less than the amount obtained in the first stage.

8.2.2 Results based on the small scale system

Once the verification of convergence in the Weymouth equation has been accomplished and validated, the obtained results have been interpreted and analyzed. It is important to highlight that the main reason why this is studied is in order to understand and quantify how much flexibility the natural gas systems provide to the power systems. As a result, it has been considered a scenario where, in the recourse stage, it is obtained 99% of the wind power expected by the forecast. Thus, the following two images will represent both power and natural gas dispatch, specifying where each amount comes from.

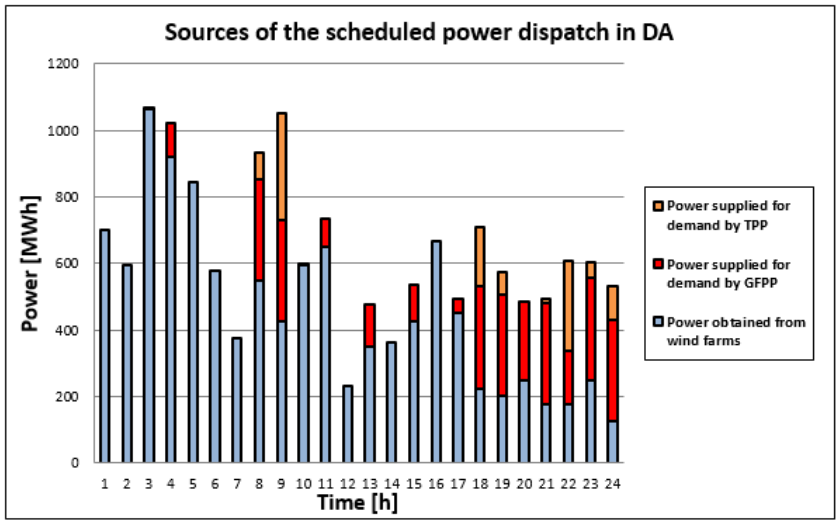

Figure 8.13: Power dispatched in DA with a 99 % of the wind expected by the forecast. Wind penetration in the first stage = 73.22 %.

Figure 8.13 illustrates for each of the 24 hours time horizon the amount of power dispatched and from which source. In the studied system, there are basically three power producers, the renewable resource (coming from the wind), the gas-fired power plant (GFPP) that uses natural gas to obtain energy and, finally, the thermal power plant (TPP) which uses the combustion of other fossil fuels to produce electricity, such as coal or petroleum.

Wind power is the primary resource to supply the demand (which in this case is always met and corresponds to the entire sum of bars of each hour). However, from this figure, it can be seen how *a priori* natural gas plays an important role in the power systems, providing flexibility in case of need. As a result, it also reflects how the system relies on GFPP to produce the extra power that the wind farms could not obtain from the wind. Lastly, the thermal power plant is only needed when any other technology can not provide energy. Thus, only when maximum capacities are reached, the system will demand energy from the TPP.

On the other hand, the following image will show the sources of the gas dispatched, also in the first stage (DA).

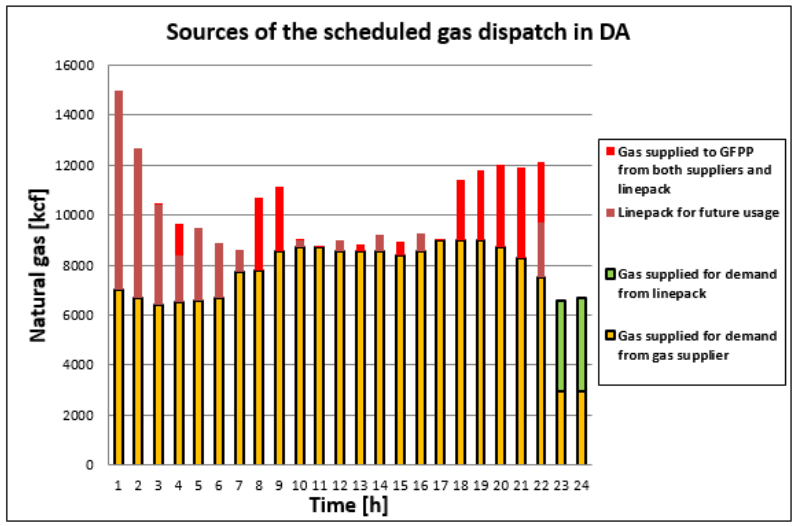

Figure 8.14: Gas dispatched in DA with a 99 % of the wind expected by the forecast.

Figure 8.14 illustrates the three different roles of the gas obtained by the gas supplier. The yellow bar represents the amount of gas supplied to meet the gas demand uniquely. Furthermore, the dark red represents the amount of natural gas supplied into the system for natural gas storage and therefore, for future usage. Finally, the bright red corresponds to all that amount of gas used to supply the GFPP. Note that, as the legend of figure 8.14 states, the amount of gas given to the GFPP can be provided from both the previous linepack in the pipelines or the gas supplier.
At the same time, the green bar shown in the illustration reflects the extra gas stored in the pipelines (linepack) that is used to meet demand. As a result, at the end of the period, the model will try to supply the demand with the maximum amount of gas stored in the pipelines, always assuring a minimum level in order to avoid depletion (equation 5.5q). Overall, it can be learnt from the graph 8.14 how the gas suppliers provide an extra amount of gas in order to add flexibility to the power systems.
On the other hand, it is also interesting to analyze the behaviour of natural gas in terms of how much flexibility can add to the power system in the recourse stage. Due to the uncertainty of the renewables, there is a need to take recourse actions to tackle situations such as the total power mismatch. Hence, the following image gives an idea about how flexible can natural gas systems be :

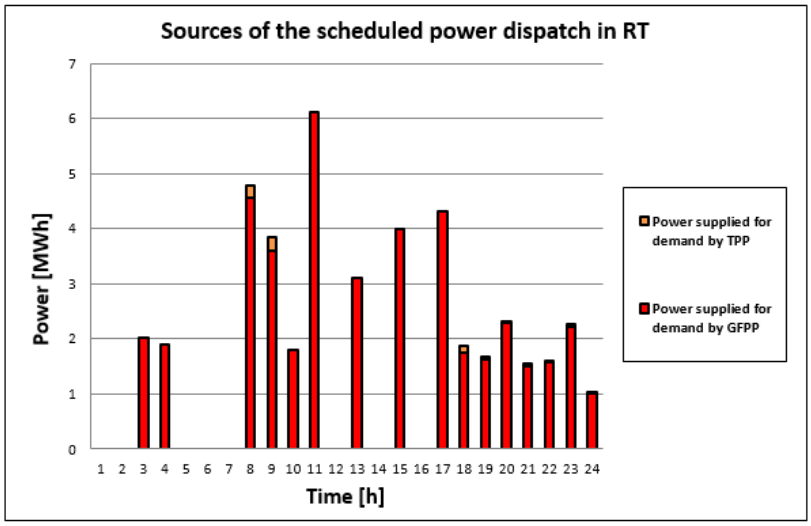

Figure 8.15: Power dispatched in RT with a 99 % of the wind expected by the forecast.

Figure 8.15 illustrates the resulting amount from the difference in the gas supplied to GFPP from both graphs 8.14 and 8.13 (note that the units of the natural gas and power are different, therefore, power conversion factors of the GFPP will be needed). As a result, the dispatched amount in the recourse stage will correspond to those adjustments needed to be able to meet demand. It also reflects that natural gas becomes the primary source of flexibility in charge of providing most of the needed amount in the recourse stage. However, GFPP are also limited by their capacity, and therefore, when increasing the total power mismatch, it can also be possible that other technologies will be needed to obtain all the adjustments needed to meet the demand (in this case, thermal power plants).

On the other hand, the following graph will show where all the adjustments of the gas provided in the recourse stage come from. As a result, it can be rechecked how useful can linepack be in the co-ordination of both power and natural gas systems:

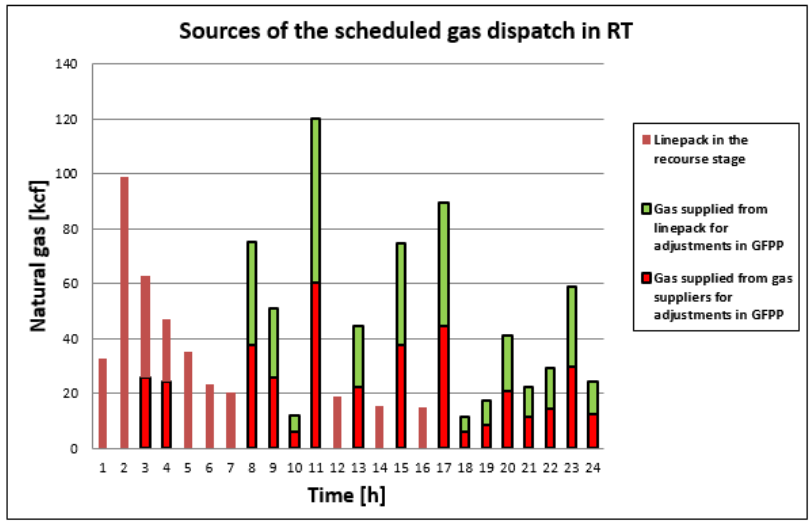

Figure 8.16: Gas dispatched in RT with a 99 % of the wind expected by the forecast.

From image 8.16 it is possible to have an overview of the scheduled gas dispatch in the recourse stage. By going back to chapter 7, where all the small scale system is described for further applications in this master thesis, table B.3 defines the wind factor obtained for the entire time horizon. As a result, by the end of the day, the amount of the incoming wind is reduced drastically compared to what it is obtained in early hours. Thus, the system relies less on renewable energy, and it is forced to use conventional power plants to meet the demand. Hence, the scheduled amount produced by these plants in the first stage increases. That is the reason why figure 8.16 illustrates that in the second stage, the system is relying more on the natural gas stored in the pipelines. However, all this linepack comes from the early hours of the day, where the gas supplier stores large amounts as it only needs to meet the gas demand, without providing almost any gas for power production in the gas-fired power plants.

As a result, this two-stage programming example can give an overview of the flexibility that linepack can provide to co-ordinated systems, power and gas in this case. In addition, before concluding this two-stage programming section results, it has also been considered the impact that natural gas has on the system when reducing the potential incoming wind. Therefore, the following image will show the share that GFPP has in the recourse stage to supply the missing demand not met form the DA

stage:

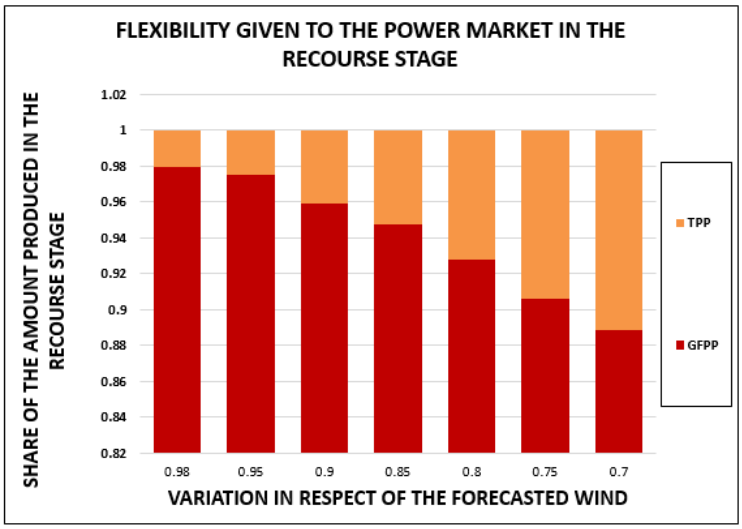

Figure 8.17: Share of power supplied by conventional power plants depending on the incoming wind in the recourse stage..

Figure 8.17 reflects the share of each of the technologies with different amounts of incoming wind. The x-axis, variation in respect of the forecasted wind, represents the factor that is multiplied to the amount expected by the forecast. However, the quantity obtained in reality will correspond to the amount in the first stage multiplied by this factor. As a result, it can be seen that the share of the gas produced by the GFPP descends when the incoming wind reduces. This behaviour makes sense as both plants, GFPP and TPP, are limited by a maximum generation. Hence, by reducing the real amount of wind obtained, the co-ordinated system will rely more on the natural gas already in the first stage. That is the reason why the production of power in the recourse stage by GFPP reduce its share when the incoming wind decreases, as more power is scheduled already in the day-ahead stage. However, it can also be seen how even if the incoming wind reduces by 30 %, the total supplied amount obtained by the natural gas corresponds to the 89 % of the total quantity produced in the recourse stage, which corresponds still to a large share over the total. On the other hand, figure 8.17 also illustrates the fact that with less mismatch of the total wind power obtained, the recourse stage relies on natural gas as the primary fossil fuel to produce electricity.

8.3 Chance constraints

This section will contain all the studied results after applying chance constraints to the co-optimization model. The software used to program the mathematical formulation is the Gurobi Python interface. Therefore all results are affected by the limitations of the software. As a result and, as it has been done through all this master thesis, the first essential thing to do is a convergence check in the Weymouth equation. Moreover, similarly to the deterministic two-stage programming, it is also important to check both first and recourse stage. Another important fact to consider is that all the explained results will be with a risk factor ($\epsilon = 0.05$) accomplishing their constraints 95 % of the times. The main reason why this risk factor is chosen to be small is that even if transmission lines, for example, can exceed their maximum capacity flow, it is important to understand the possible consequences of exceeding its maximum capacity for so long. If a line is over exceeding its maximum capacity for a long period of time, it will overheat and thus, the longer it stays, the higher chances that the line will trip. Furthermore, the time that the line needs to trip is measured in minutes, so this matter needs to be accounted for when applying CC. Furthermore, the trip of a line can provoke a cascade failure with fatal consequences. [BCH12].

8.3.1 Solution Check

For the solution check of the CC optimization problem, the same error equation defined in 8.2 has been used. As a result, the obtained error for the DA stage is represented in the following image:

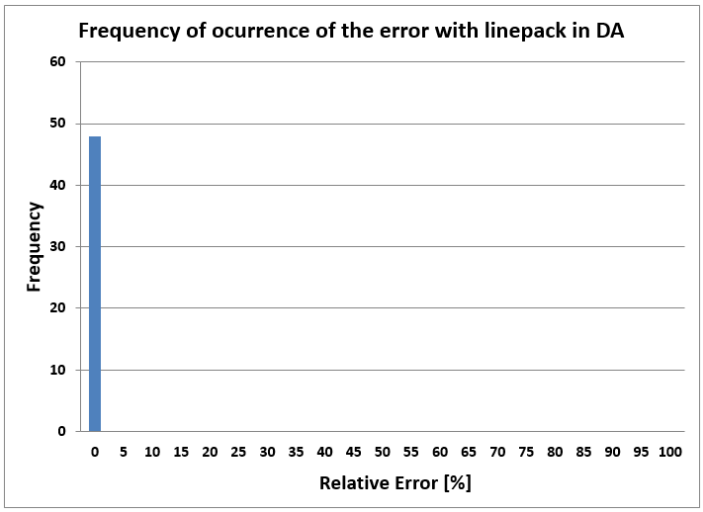

Figure 8.18: Solution check of the CC-OPF in the DA stage.

Figure 8.18 shows the relative error of the 48 solutions obtained (one per pipeline per 24 hours time horizon). It illustrates that all the relative errors studied are around 0 %, validating the relaxation applied as the system behaves almost as an equality constraint. As a result, the error obtained by equation 8.2 is $1.17 \cdot 10^{-7}$%.

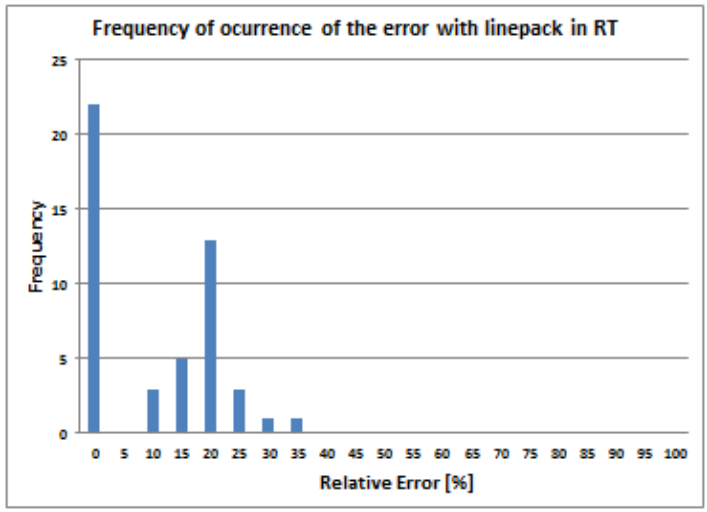

Figure 8.19: Solution check of the CC-OPF in the RT stage.

Referring to the solution check of the recourse stage of the CC-OPF, the numbers obtained are not as desirable as figure 8.18. Image 8.19 shows that adding uncertainty into the problem leads to different behaviour of the entire system, increasing the relative error. In fact, only 22 times out of 48, the left-hand side of the Weymouth equation is equal to the right-hand side. Nevertheless, after computing also the error formula from equation 8.2, it is obtained a total of 1.89 %. It can actually make sense that the system has more difficulties in acting as if the Weymouth equation was an equality as uncertainty is added and probability functions (Gaussian with 0 mean and standard deviation σ) are included in the constraints (as they are reformulated analytically).

8.3.2 Results based on the small scale system

8.3.2.1 Risk factor ϵ

As stated in previous chapters of this master thesis and also in [Roa16], the ϵ or risk factor determines the percentage given to a specific constraint to fulfil it, allowing ϵ times an overtake its boundaries. As a result, this section will focus on the impact of this value into the entire system, analyzing its influence on the total system costs. In order to do it, it has been chosen to analyze the total system costs by varying in 0.05 the risk factor, from almost a 0 value to 0.5. The function where it is evaluated this probability corresponds to the *cumulative distribution function*:

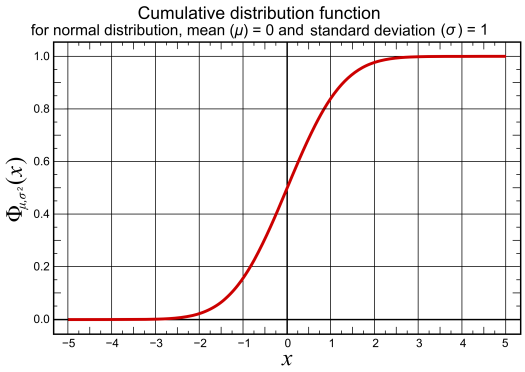

Figure 8.20: Cumulative distribution function.

Besides, by considering any of the analytical reformulations developed in this master thesis, such as equation 6.15b, it is explained the reason why the ϵ is evaluated until 0.5:

$$p_{i,t}^{DA} \leq P_i^{MAX} - \Phi_{\mathbb{P}}^{-1}(1-\epsilon)\big|\big|\alpha_{i,t}\sigma\big|\big|, \quad \forall i,t, \tag{8.5a}$$

As a result, by considering equation 8.5a, the main reason why the cumulative distribution function is not evaluated in a value higher than ϵ=0.5 is that it will result in a negative value (note that Φ_{μ,σ^2}(1-ϵ), see figure 8.20). Therefore, as it is stated in [Roa16], the second term of the right-hand side equation has to be always positive. Hence, with the negative sign in front, it will always lead to a reduction in the available capacity.
The following figure represents the different total system costs depending on the chosen risk factor value:

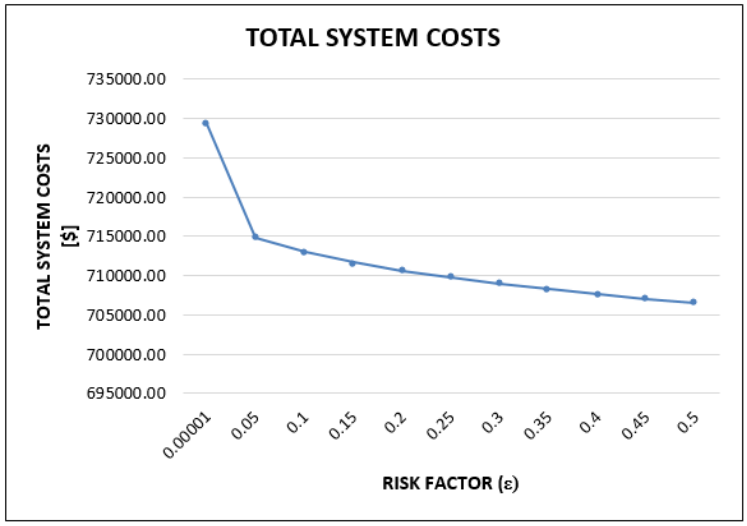

Figure 8.21: Total system costs depending on the ϵ.

Figure 8.21 illustrates a descending trend in the total system costs of the co-optimization problem whenever the ϵ value increases. These values are expected as with lower risk factor values, the system is behaving more conservative, and thus, the constraints are accomplished with higher frequency. As a result, when this parameter is increased, the system costs are reduced until reaching 0.5, where it gets the lowest

possible costs. The reason why the system is not evaluated in ϵ=0 is that the value of the cumulative distribution function will result in infinity (see figure 8.20). Therefore, it has been chosen a small enough value to show the steep increase that the total system costs will experience in case it is considered a full conservative case without any violation of the constraints. Similarly, the following image will present the total wind penetration depending on the risk factor.

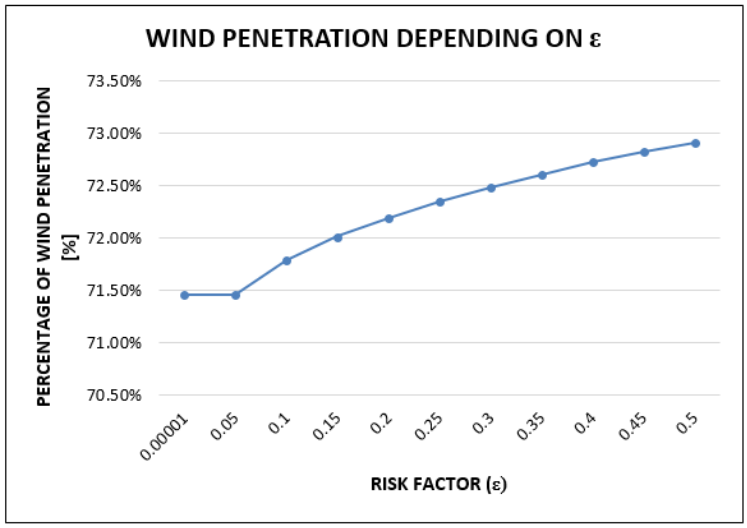

Figure 8.22: Scheduled wind penetration in the first stage (DA) depending on the value of ϵ.

Figure 8.22 illustrates the variation of expected wind in the first stage (in the form of wind penetration i.e. total wind power produced divided by the total power demand), depending on the value of the risk factor. As a result, due to the uncertainty of the wind obtained in the recourse stage, the total system will react to the conservativeness of the problem, dispatching more power from the wind farms in those cases where the probability of meeting certain constraints is low (close to 0.5). In consequence, the higher the risk parameter is considered, the less constrained the problem will be, resulting in a more dispatched wind power production in the first stage. However, the range of variation corresponds to approximately 1.5 %, showing that even when the problem is less conservative, the variation in the scheduled wind power production does not reach extreme values compared to the most constrained case.

8.3.2.2 Linepack analysis

This section contains the linepack results after simulating the model with an $\epsilon = 0.05$ and a standard deviation $\sigma = \sqrt{200}$ (considering a fluctuation of 100 [MWh] per wind generator, and following the equation described in 6.7a). Hence, the following image represents the linepack behaviour for both first and recourse stage:

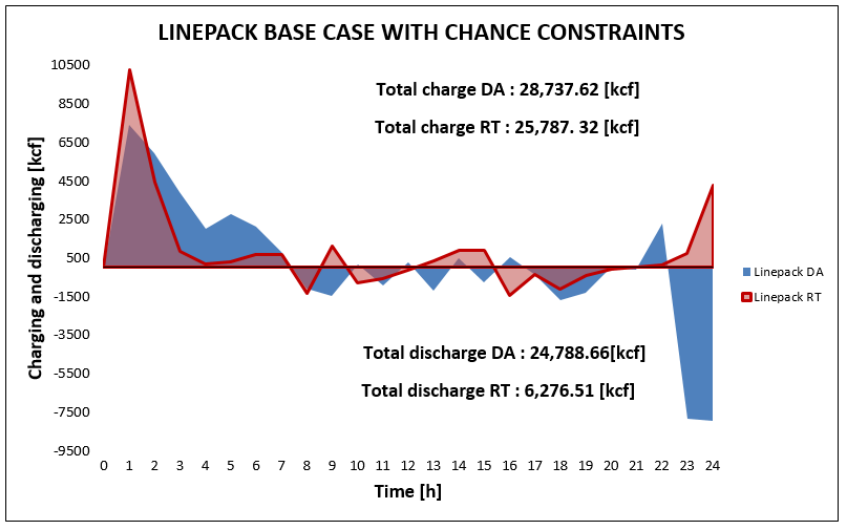

Figure 8.23: Linepack behaviour of the entire system for both first and recourse stage.

Accounting for both pipelines (remember that these results are applied to the base case explained in chapter 7), figure 8.23 illustrates the charge/discharge that the entire system experiences throughout a day. It is indeed interesting to analyse the variations between both stages, as they differ significantly for one stage to another. As it is also shown in the picture, the red function represents the recourse stage charge/discharge of natural gas and the blue one, the day ahead. In the beginning, both stages experience a significant charge in the pipelines, followed by some fluctuations in between before it is reached the last two hours. The linepack in DA suffers a considerable drop in order to supply the gas demand in their last two time periods. However, after some fluctuations in between, the recourse stage decides to still charge the pipelines for the last hours even though it still has large quantities stored. At the end of the time horizon, the balance in the first stage corresponds to a

remaining amount of 3,948.96 [kcf] (note that the word *remaining amount* is in italics because the first stage only schedules the optimal amount, considering all the data is correct without the need to apply corrections later). On the other hand, in the recourse stage, the system decides to store more natural gas in the pipelines, reaching the amount of 19,510.81 [kcf] by the end of the time horizon.

8.3.2.3 Standard deviation of the total wind power mismatch $\Omega \in \mathcal{N}(0, \sigma^2)$

In previous sections of this master thesis, it has been outlined the two different approaches when using chance constraints, sampling or assuming known distribution. As a matter of fact, this document has focused on solving chance-constrained problems assuming known the distribution (normal) and, as a result, being acquainted with the mean ($\mu = 0$) and standard deviation ($\sigma = \sqrt{200}$), being 200 the obtained value from the covariance matrix, used to quantify the σ (refer to equation 6.7). Therefore, this section aims to show the impact that the standard deviation has in the described problem in chapter 7, quantifying the shares of wind penetration and power produced by both GFPP and TPP. Hence, the following image gives an idea of the importance of this value in terms of the shares of the different power production sources:

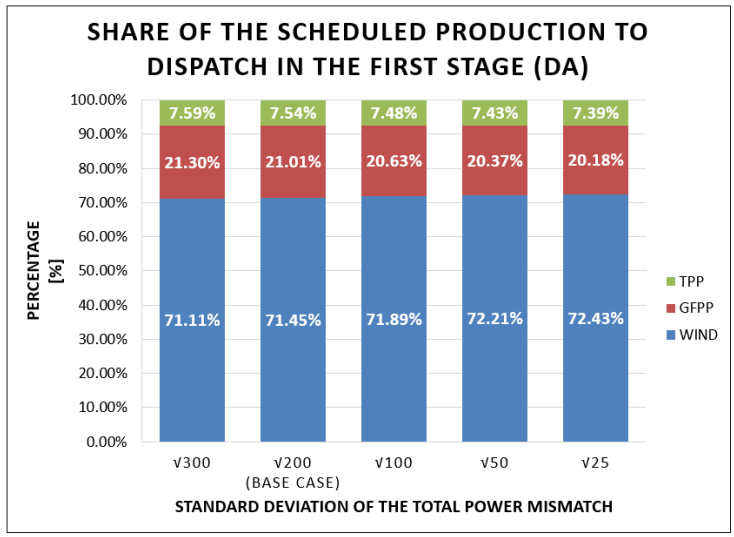

Figure 8.24: Share of power suppliers in the 1^{st} stage by varying the standard deviation of the total wind power mismatch.

Figure 8.24 depicts the total shares of the different sources used to supply the power demand in the first stage. Wind power is, by far, the most used to obtain electricity. Furthermore, the bar chart also illustrates the fact that the larger standard deviation considered, the less power will be obtained from the wind farms. This fact makes sense as the larger fluctuations obtained in the system, the more uncertainty it will bring. Note that in the co-optimization system, natural gas is also used to supply the GFPP to produce the extra remaining possible amount to meet the demand. It is essential to highlight that not all the rest of the power needed is supplied by the GFPP as power plants are limited with a specific maximum capacity and in co-optimization systems, gas is also used to meet the gas demand of the system.
On the other hand, it is also interesting to know which power plants are the most used to provide flexibility to the system in the recourse stage. As a result, the following figure will give an idea (also depending on the value of the σ):

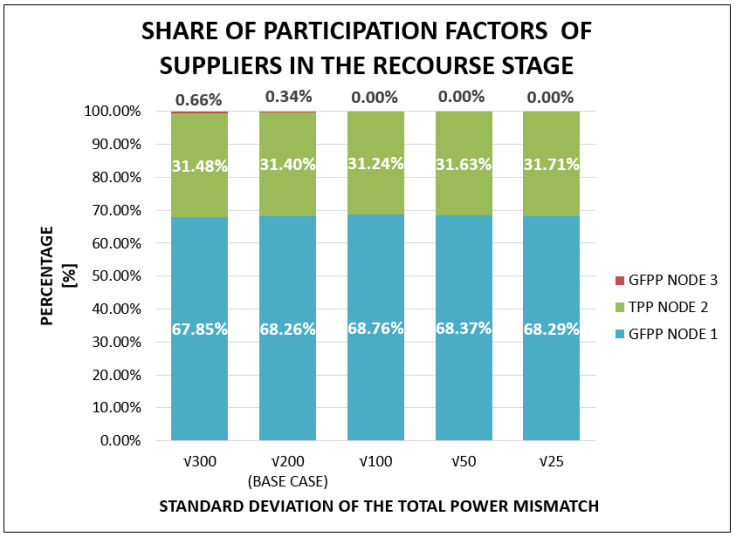

Figure 8.25: Share of the participation factors correcting the mismatch from DA (Day Ahead).

Throughout the entire time horizon, corresponding to 24 hours, the GFPP located in node 1 is the power plant taking more action compared to the others in the recourse stage. This fact can also be understood as firstly, the price of the natural gas results in much lower than the cost of generating one unit of energy in the TPP. However,

even if the price of the gas is lower than in the other conventional power plants, it is crucial to bear in mind the fact that each GFPP possesses a specific conversion factor, in charge of relating the amount of natural gas needed to obtain one unit of power. Hence, the conversion factor from the GFPP located in node 1 has a lower value compared to the one located in node 3. This means that with less amount of gas, the same unit of energy can be produced as in the GFPP situated in node 3. This graph also proofs that natural gas can provide flexibility to balance the mismatches obtained in the recourse stage. Therefore, the more precise the forecast wind is, the less production of any conventional generator will be needed in the recourse stage.
Finally, the total system costs depending on the value of the standard deviation are shown in the following image:

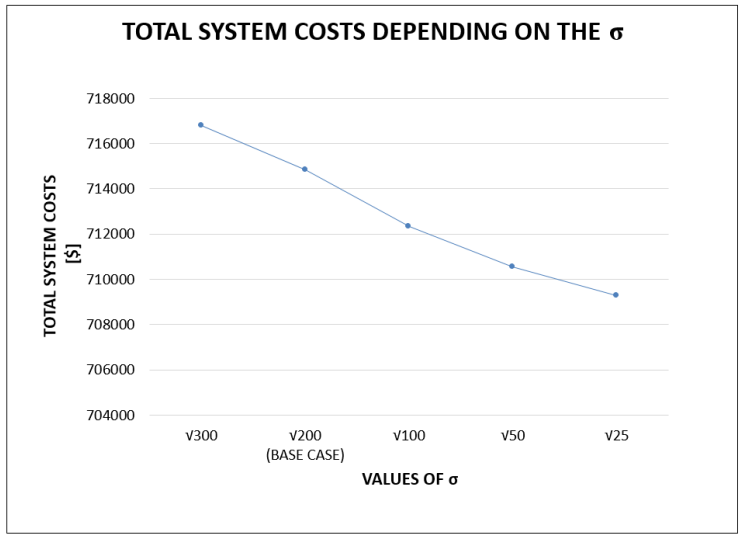

Figure 8.26: Total system costs .

To conclude this study, figure 8.26 illustrates a descending total system costs, depending on the error of the forecast wind. This trend is the expected as when obtaining lower fluctuations in the total power mismatch; less recourse action will need to be taken and thus, fewer system costs to the entire system.

8.3.2.4 Variation in the cost of the gas

Similarly to the previous study, another sensitivity analysis will be developed in order to understand the impact of the gas cost in the entire system, analyzing its reactions and thus, the recourse actions taken to cope with the changes.
As a result, in the first place, the following image will illustrate the share of the productions in the DA stage in order to be able to identify which variables will result affected:

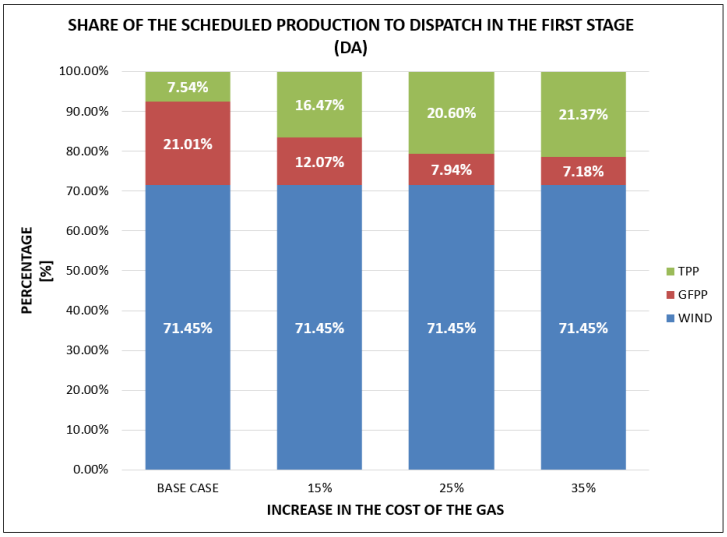

Figure 8.27: Share of power suppliers in the 1^{st} stage by varying the cost of the gas
.

The first thing that illustration 8.26 depicts is the fact that no matter the cost of the natural gas, the values of the scheduled dispatch of wind power will remain fixed entirely. Therefore, there is no impact on wind power production by varying the cost of natural gas, obtaining a total penetration of 71.45 %. However, even if the case study is a co-optimization problem between power and gas systems, the share of the GFPP will considerably decrease. As a result, all the lost amount by this conventional power plants will be taken by the TPP, raising its share in the system when the cost of the gas increases. It is also worth mentioning that the first variations result in more drastic changes. Afterwards, those variations smooth when the decrease in the cost of the gas gets considerably high.

Following the same procedure as before, the next step is to show how the participation factors in the recourse stage get affected by the variation of the natural gas cost. Hence, the following image gives an idea of it:

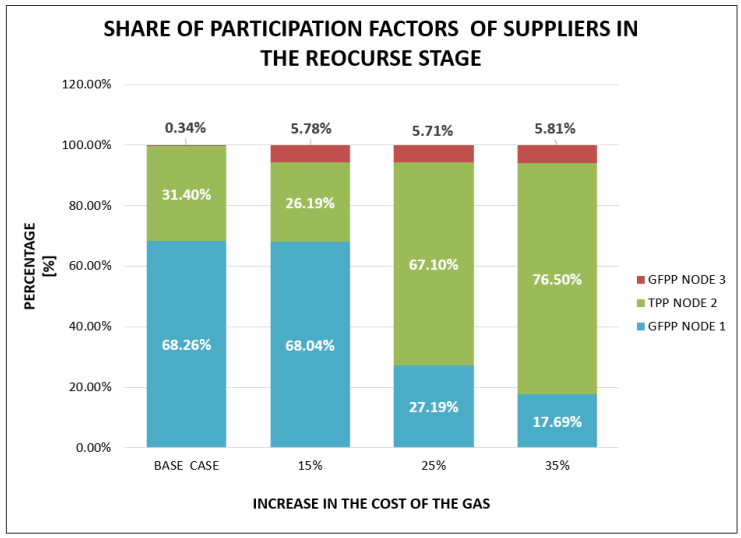

Figure 8.28: Share of the participation factors by varying the natural gas cost .

By increasing the gas price from 0-15 %, still, the main actor supplying in the recourse stage is the GFPP located in node 1. Moreover, there is a decrease in the production of power from the TPP, possibly since it increases its production during the first stage. The main driver for such behaviour corresponds to the price for producing one unit of power in the GFPP. Figure 8.26 illustrates that even if the price of the natural gas is increased by 15 %, the plant located in node one will be the leading supplier for flexibility. The reason why this happens is that the cost of producing one unit of power will be slightly less than the cost of the TPP. Nevertheless, the GFPP located in node three will reduce its power production considerably, even if the graph might seem that it took more relevance in the production of the recourse stage. Combining both graphs 8.29 and 8.28, it can be understood that also due to maximum capacities, some of the most expensive power production plants will, at least, have specific participation in the production of power. However, increasing the natural gas costs to levels where the unit of power produced by GFPP exceed the cost of the unit of power produced by TPP, the system will be undoubtedly sure the

latter one to be the main supplier of flexibility, reducing the share of participation of the GFPP considerably.

Lastly, the following figure will represent the total system costs due to the variations in the gas price:

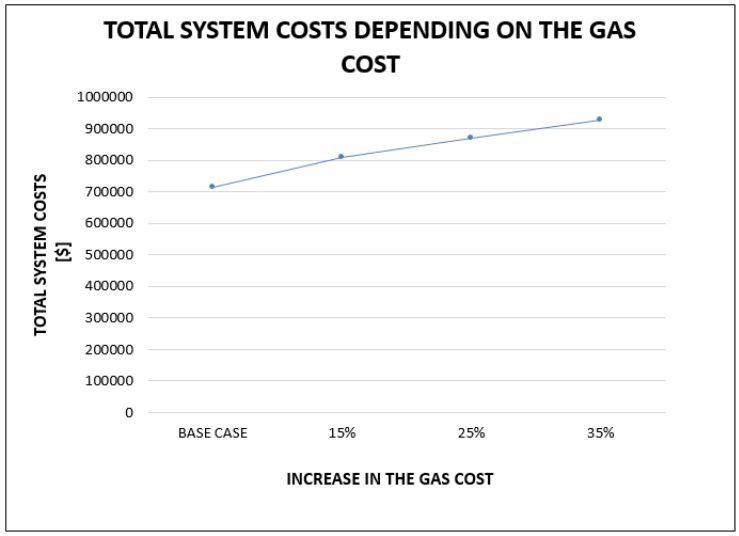

Figure 8.29: Total system costs.

Figure 8.29 represents the total system costs depending on the cost of the gas. As a result, the more expensive the cost of the natural gas is, the higher costs the system will obtain.

8.3.2.5 Variation in the conversion factors (ϕ) of the GFPP

Even if it is a fact that the cost of natural gas can be lower compared to other commodities [ULD07], it does not mean that in order to produce one unit of power it is therefore needed one unit of natural gas. The conversion factors of the GFPP play an essential role in the flexibility given to the power systems. This factor, in simple words, corresponds to the amount of gas to supply in order to generate a unit of power. As a result, depending on the needed amount, it might be possible that the cost of producing electricity in GFPP may be higher than other conventional power plants.

The same study will be developed to understand the influence of this factor concerning the results obtained in the entire system.

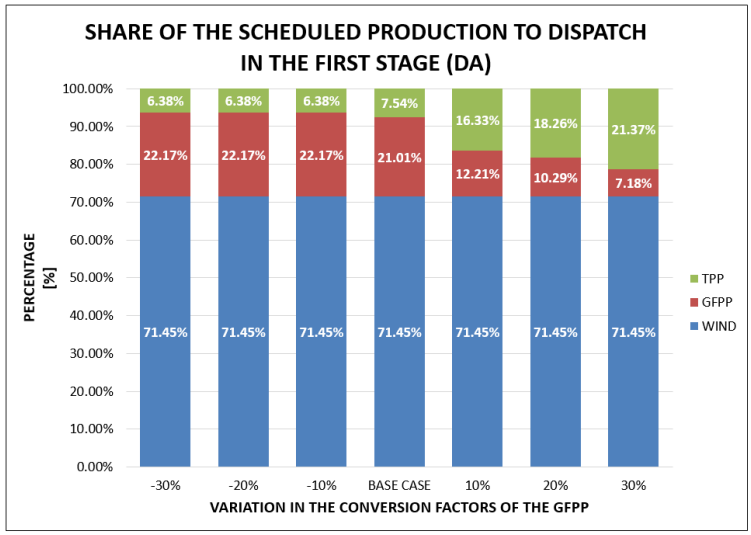

Figure 8.30: Share of power suppliers in the 1^{st} stage by varying the conversion factors of the GFPP.

Figure 8.30 depicts how the share of suppliers vary depending on the value of the conversion factor. Even if in the base case there are two gas-fired power plants, it is considered that the variations shown in figure 8.30 apply to both. It also illustrates that the value of the conversion factors does not affect the wind penetration, obtaining for each of the different situations a share of 71.45 %. Moreover, it also reflects the behaviour of the different conventional generators, varying their share, depending on the value of the conversion factors. As a result, the higher it gets, the more expensive it becomes to produce one unit of power, decreasing the share of GFPP and, on the other hand, increasing it for the TPP. However, due to capacity limitations of this plants, when these factors are decreased (the unit of power in those plants becomes cheaper), the total share remains the same (increasing the participation of the GFPP, compared to the base case). On the other hand, by analyzing the share of the participation factors in the recourse stage, the following graph is obtained:

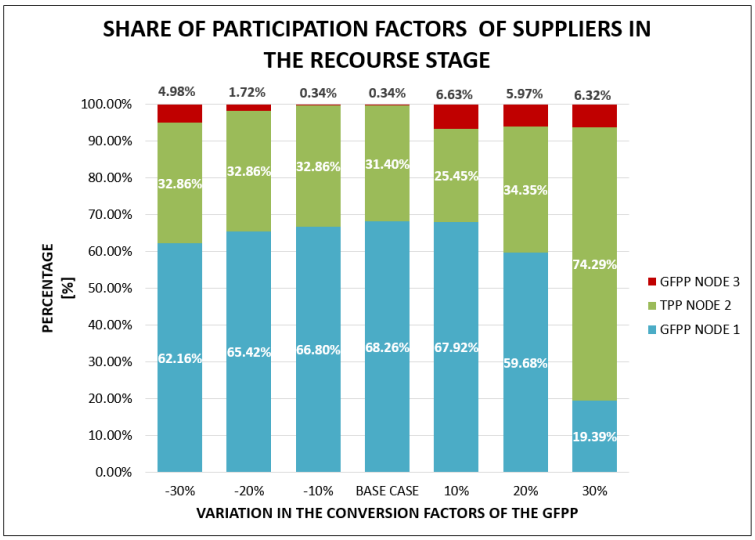

Figure 8.31: Share of the participation factors by varying the conversion factors of the GFPP.

The participation factors shown in figure 8.31 illustrate, in a way, the repercussions of having a high or low conversion factor. To start with, when decreasing them, the total participation of GFPP (without differentiating them) corresponds to the same amount. Note that the participation factor of the TPP remains constant for conversion factors lower than the base case. In order to understand this, it is also important to analyze at the same time figure 8.30. One of the main drawbacks is the capacity limitations, as due to an increase in the share in the scheduled amount in the first stage, it limits the possibility to increase the participation factors in the recourse stage. On the other hand, by increasing the conversion factors, image 8.31 illustrates how the TPP becomes essential to provide flexibility in the recourse stage. Even if the conversion factors are increasing, in the case of GFPP 1, its value does not increase enough to exceed the cost of producing one unit of power. Therefore, this is the reason why when increasing 10% and 20%; still, the participation factor of GFPP is higher than TPP. Lastly, when the conversion factor is increased by 30 %, the TPP becomes the main supplier in the recourse stage by being the cheapest generator. Similarly to the results mentioned previously, the capacities of the plants still limit both stages, preventing from increasing their production and thus, reducing the total system costs.

In addition, the following illustration will show the variation in the total system costs due to different fluctuations in the conversion factors:

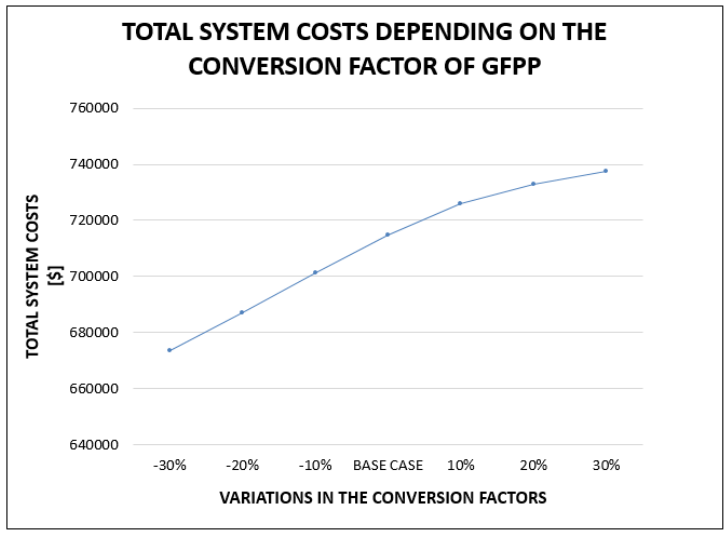

Figure 8.32: Total system costs.

As a result, and also expected, figure 8.32 shows how the total system costs reduce when the conversion factors reduce, which means a lower cost for a power unit produced in the GFPP. However, the higher the values are, the more expensive will result in the total system costs.

CHAPTER 9

Discussion

This study aims to analyse the co-ordination between power and natural gas systems under uncertainty by using chance-constrained programming. It is true that lately, due to the increase in the construction of new gas-fired power plants, the idea of a co-optimization between power and the natural gas system has become more plausible [Rub+08]. However, the coupling system is still an ideal benchmark with a large potential for further study [Sch+19] and [Zlo+17]. It is true though that all the work developed in this master thesis could not be done without the existence of an entity operating both power and gas systems, as it is stated in both [Sch+19] and [Pin+17]. As a result, by assuming that the transmission system operator (TSO), i.e. Energinet.dk, is operating both systems, the first step was developing and implementing a deterministic unidirectional model. The existence of a quadratic constraint (Weymouth equation explained in 5.2k) has led to the application of relaxation techniques in order to convexify the problem. Hence, before any simulation was done, a convergence check was needed to assure that the system was behaving according to what is doing in reality. It is therefore worth mentioning that, the error calculated in the convergence check result in 0 for all those cases where linepack was accounted for. On the other hand, when the system was considered without linepack, the convergence check results were not as desirable. It is thought that a potential reason for this behaviour could be the addition of an extra variable, the linepack. Even if the problem becomes more constrained by the addition of new constraints, on the other hand, the co-ordinated system can benefit from a new variable that enables storing the natural gas not needed inside the pipelines. Consequently, this gas can be further used, reducing the oversupply of natural gas and allowing to extract an amount whenever it is needed. Moreover, the example used to implement the one stage unidirectional deterministic case, which corresponded to a three nodal power and gas problem, showed that the behaviour of the charge and discharge of the linepack in the system was following, to some extent, the same trend. Thus, no matter the sen-

sitivity analysis performed afterwards, the pipelines were charging with natural gas by the first seven hours of the day (with more or less quantity), experiencing some minor fluctuations in between and finally, before the end of the day, discharging large amounts. One possible answer for such behaviour is that the *leftover* natural gas from the supplier could be stored without problems. Therefore, if this could be done, suppliers might oversupply in those periods where natural gas is not necessary for power production (i.e. high incoming wind) and afterwards, store all the quantity left after meeting demand and store it into the pipes. Besides, it was also proven that the linepack behaviour varies and adapts to different situations, as it was seen in the different study cases.

Moreover, the second step of this document was to implement the same case into a two-stage unidirectional deterministic case, where it could be studied the behaviour of the system facing a first and a recourse stage. Following the same procedure, as mentioned in the last paragraph, before any study, a solution check needed to be performed to check the accuracy of the relaxation. As a result, for both stages, the obtaining error was 0, assuring that the system is behaving according to reality, and thus, the SOC relaxation was validated. Afterwards, the system was implemented into the invented small scale system. The system showed good results for DA in terms of co-ordination between the natural gas and power systems, proving that in case of needing extra power, the first source (after the wind power generation) was the gas-fired power plants or linepack and afterwards, the thermal power plants. Referring to the recourse stage, the main source of flexibility added to the systems came from the GFPP. Figure 8.17 showed a descending share in the recourse stage with the lower incoming wind. However, it is also important to highlight the fact that this descends due to the supply given in the DA stage.

Finally, the last part of this master thesis was to apply chance constraints to the two stages deterministic problem, adding thus uncertainty in it. The program used to solve such problems was Gurobi Python. Therefore, all solutions are subject to the program limitations. The results obtained during the solution check were not as good as desired. It is important to highlight although that the error obtained in the first stage results in 0 whereas in the recourse stage, when the uncertainty of renewables was added into the system, the total error results in a higher value, however, still accepted. Regarding the risk factor ϵ, it has been proven that the lower the value, the higher total system costs due to conservativeness [BCH12] and [Roa16]. Due to the cumulative distribution function showed in image 8.20, the risk factor can not be

0 (as the result will be infinite) neither superior than 0.5. As stated in [Roa16] the second term of the right-hand side equation 8.5a needs to be always positive (as with the negative sign in front, the entire term will result in a negative value). Another important fact to highlight is the graph shown in 8.22. The more conservative is the problem, the less scheduled wind in the first stage. A potential reason why this is happening can be since with lower values of ϵ, the system is following the constraints more times, and in consequence, the results need to be conservative to meet demand and also boundaries or constraints. However, for larger values, image 8.22 illustrate an increase (small) in the percentage of wind penetration. Moreover, related to the linepack results, the plot showed in figure 8.23 illustrate the total linepack of the entire system in both DA and RT. The shape and the trend described by the blue area, the one corresponding to the DA, showed the same dynamics as all the rest of the plots in this document. Nevertheless, it was a bit surprising the results obtained for the recourse stage as the system is charging a lot the pipelines with natural gas during the first 2-3 hours of the day, experimenting small fluctuations in between and finally charging slightly more. This kind of linepack behaviour has not been seen before in this paper, and the results are unexpected as the system is not obtaining in the recourse stage the entire potential of the linepack. The last studies conducted to the CC programming were three sensitivity analysis where three parameters were modified to study its behaviour (i.e. standard deviation, cost of the gas and variation in the conversion factors of the GFPP. The only study where the wind penetration alters its incoming amount into the system corresponds to the standard deviation of the total power mismatch. As a result, the total share in the first stage differs slightly. It states a wind penetration of around 71-72.5 % with more or less the same shares for the GFPP and TPP. In addition, similarly occurs with the shares of participation factors in the recourse stage, where the GFPP located in node one is by far the most used to supply flexibility. Thus, the highest total system costs will correspond to those values of high standard deviation, corresponding to significant uncertainty. On the contrary, low values of standard deviation will result in lower costs.

On the other hand, related to the increment of the gas price, wind penetration is the only value that will remain the same. It makes sense as the uncertainty of the total power mismatch (set as $\sqrt{(200)}$) has no relation with the variation in costs (as the cost of a renewable source is considered to be null). However, the more expensive the gas is, the more the system will rely on the TPP. Referring to the participation factors in the recourse stage, the TPP will provide the most flexibility in the recourse

stage as its cost of production will become cheaper than the new cost of natural gas. Also, due to limitations in the capacities of the different power plants, it might not be possible to adequately supply the needed amount and thus, increase the share of the most expensive ones in those cases where the maximum capacity of a power plant is reached. The total system costs will increase when the marginal cost of the gas increases as well.

Finally, the last result to be studied is the conversion factor of the GFPP. The main problem with this value corresponds to the limitations of the maximum capacity of the plants. As shown in figure 8.30, when reductions of these factors are made, which means that the amount of gas to produce a unit of electricity is decreased. However, with larger capacities in the GFPP, these value could increase, obtaining a reduced total system costs.

On the other hand, when it comes to an increase of these values, the share of the scheduled amount to produce in the first stage by the GFPP reduces considerably, reaching its lowest value with the highest increase. Similarly, something happens with the share of the participation factors of suppliers in the recourse stage. As stated before, for reduced factors, the GFPP endures capacity limitations, preventing them from increase their share in the recourse stage. However, when increasing their conversion factor at around 10-20 %, the total amount of natural gas needed to produce 1 unit of power, still results cheaper that in TPP. Nevertheless, the same does not occur with the last value, where the TPP results in the cheapest conventional power plant increasing its share in the recourse stage considerably.

CHAPTER 10

Conclusion

To summarise, this study has investigated the effects of adding uncertainty in a co-optimization system between power and natural gas. Furthermore, it has also accounted the uncertainty provided by the wind in terms of producing power and the application of chance constraint to account the total power mismatch, assuming it follows a normal distribution with mean (μ=0) and a specific standard deviation (σ). Hence, the concluding remarks are as follows:

10.1 Unidirectional deterministic implementation. One stage

- Without considering linepack in the system, the convergence check obtains a total error of 3.03 % when the described mathematical formulation is applied to the small scale system explained in chapter 7.
- The model described without linepack results in being sensitive to the input parameters of the described case, as by changing some of the parameters in the pipeline, the convergence check error is reduced to 2.24 %.
- The more error obtained without linepack in the system, results in lowering the total system costs, from 6.89 $\cdot 10^5$ [$] in the base case applied in chapter 7 to 6.94 $\cdot 10^5$ [$] in the modifications made in section 8.1.1.
- When linepack is introduced into the system, the convergence check obtains better results, a total error corresponding to 2.24 $\cdot 10^{-7}$%.
- It has been proven that linepack provides flexibility to the studied case explained in chapter 7, as it modifies its profile in the pipelines in order to provide flexibility to the power system in case of need. In order to assure this statement, two

different examples altering the incoming wind through the day and the demand of natural gas were applied, obtaining different linepack profiles adapting to the necessities of each of the study cases.

10.2 Unidirectional deterministic implementation. Two stages

- The two-stage mathematical program with linepack has shown great results in terms of convergence check in the Weymouth equation, obtaining a total error for both stages of 1.44 $\cdot 10^{-5}$%. Assuming that the amount of incoming wind in the recourse stage corresponds to 99 % of the forecast amount, it has also been obtained a wind penetration of 73 % for the first stage while 72.5 % in the recourse one.
- Natural gas systems (both GFPP and linepack) provide flexibility (to both DA and recourse stage) to the power systems whenever extra electricity is needed.
- Whenever incoming wind reduces considerably compared to the forecast amount, natural gas still leads in providing flexibility to the power systems (both DA and RT stages). Capacities of the power plants are limitations to fully provide electricity to the power system whenever it is required.

10.3 Chance constrained programming

- The errors obtained in the convergence check results in 1.17 $\cdot 10^{-7}$% for the DA stage and 1.89 % during the recourse stage showing that uncertainty may bring inaccuracies in the Weymouth equation.
- The higher the risk factor ϵ, the lower total system costs as the system becomes less conservative.
- The higher the risk factor ϵ, the higher wind power scheduled in the first stage.
- During the recourse stage, the linepack profile in terms of charging/discharging in the pipelines can modify its behaviour considerably compared to the results scheduled in the DA stage.

- The larger the standard deviation of the total power mismatch, the less wind power scheduled in the first stage. As a result, with the less incoming wind, the total system costs that, in this case, depend uniquely on the DA values, will increase. Moreover, when the standard deviation increases, natural gas provides flexibility to the power system always limited by its maximum power production. Besides, the GFPP to be able to add flexibility into the power systems, it needs to assure that the unit of power produced (cost of natural gas·conversion factor) is lower than the cost of the production of a unit of power of the other conventional power plants.

- The lower the standard deviation of the total power mismatch, the less uncertainty is added into the system and thus, the lower total system costs.

- Neither the cost of the gas nor the variation of the conversion factors of the GFPP will affect the scheduled amount in DA of the wind power production. This makes sense indeed as it is considered that the marginal cost of the power obtained from renewable sources is 0.

- The lower the conversion factor of the GFPP is, the higher share they will obtain in the total production to meet demand. It, therefore, makes sense that with a lower conversion factor, the total system costs reduce.

Future work will involve the implementation of a larger scale scenario. As a result, it will be interesting to analyse the behaviour of the entire system after applying chance constraints when more nodes, generators and interconnections are present. In addition, next step will be to apply chance constraints using the approximation via samples, thus generating large amounts of scenarios in order to build the probability distribution function, instead of assuming it known as it has done in this master thesis. Moreover, further study on equations 5.6q and 6.12h to investigate deeply how to transform them analytical will also have been done and compare the obtained results with the ones from this master thesis. Lastly, it will also be interesting to study different approaches to add flexibility to the gas system from the excess of wind power. [Göt+16] focus on the fact that how renewable electric energy can be transformed into natural gas (methane) by using differnt processes of electrolysis (with efficiencies of 70 %) and afterwards, methanation (with a 78 %) obtaining an overall effiency of power to gas (P2G) of 55 % (Sankey diagram, without considering heat losses cited in [Göt+11]).

APPENDIX A

Solution checks for different values of ϵ

The errors mentioned in the following graphs represent the values obtained by using equation 8.2

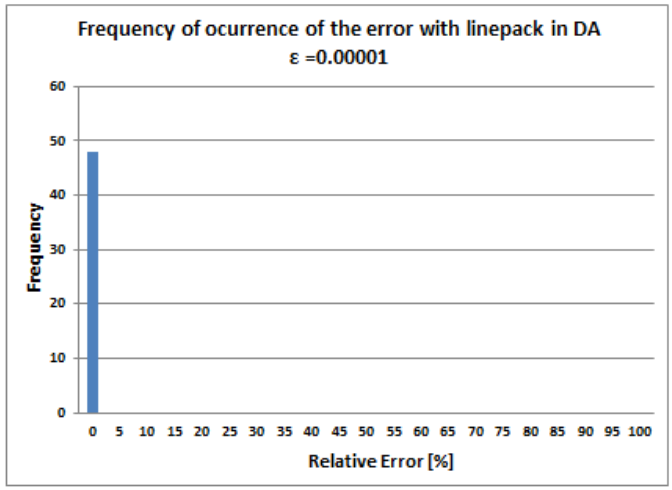

Figure A.1: Solution check of the CC-OPF in the DA stage with $\epsilon = 0.00001$. Error = 0.37 %.

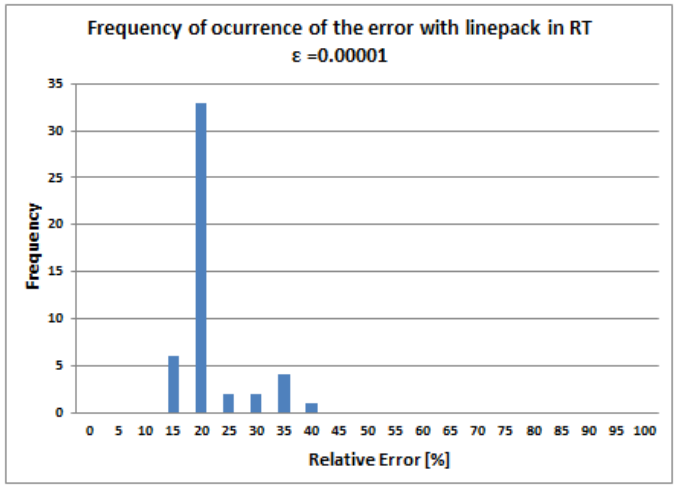

Figure A.2: Solution check of the CC-OPF in the RT stage with $\epsilon = 0.00001$. Error $= 2.85$ %.

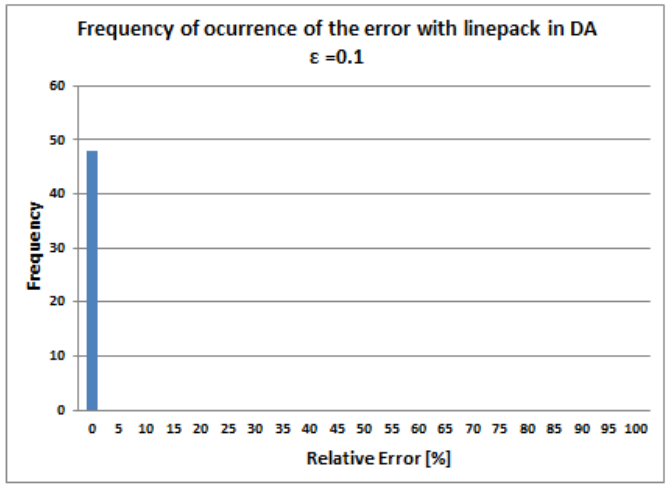

Figure A.3: Solution check of the CC-OPF in the DA stage with $\epsilon = 0.1$. Error $=1.43 \cdot 10^{-5}$%.

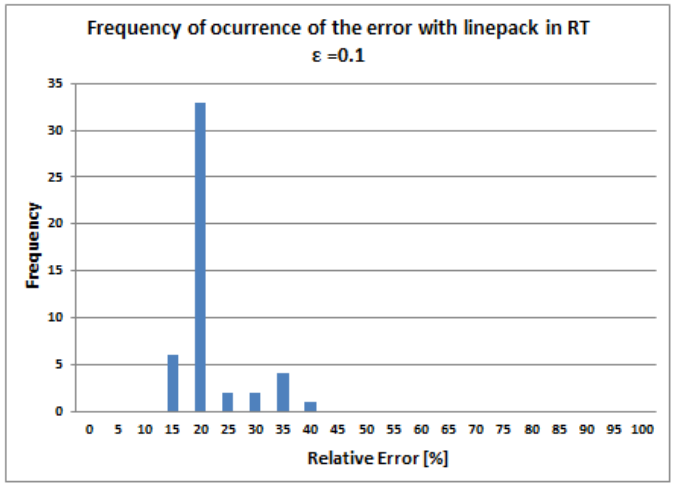

Figure A.4: Solution check of the CC-OPF in the RT stage with $\epsilon = 0.1$. Error $=2.96 \cdot 10^{-5}\%$.

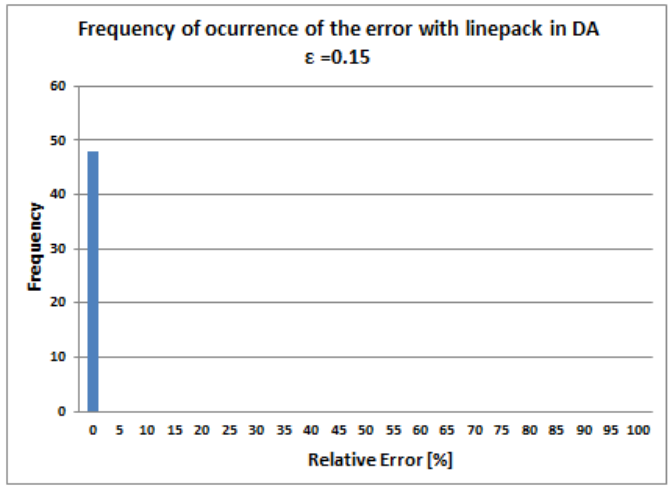

Figure A.5: Solution check of the CC-OPF in the DA stage with $\epsilon = 0.15$. Error $=$ 2.95 %.

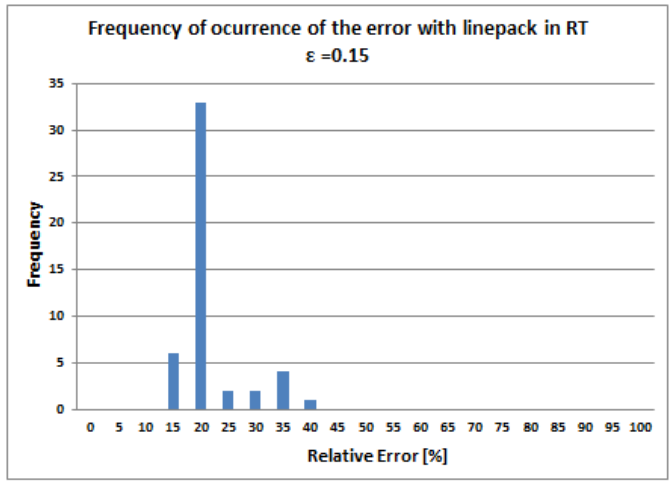

Figure A.6: Solution check of the CC-OPF in the RT stage with $\epsilon = 0.15$. Error $=9.60 \cdot 10^{-6}\%$.

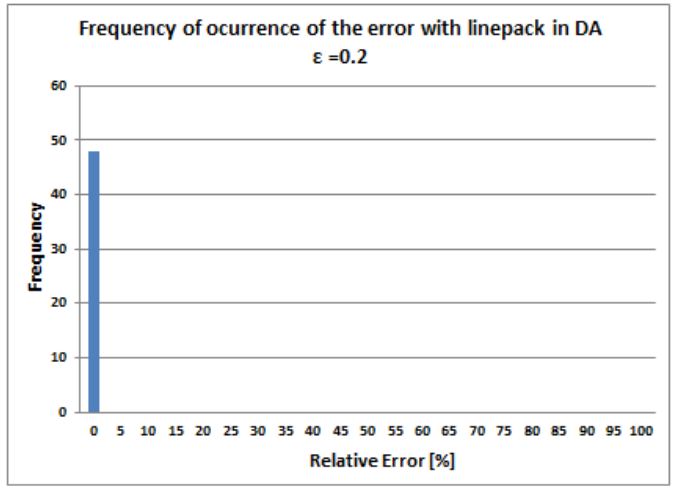

Figure A.7: Solution check of the CC-OPF in the DA stage with $\epsilon = 0.2$. Error $=7.5 \cdot 10^{-6}\%$.

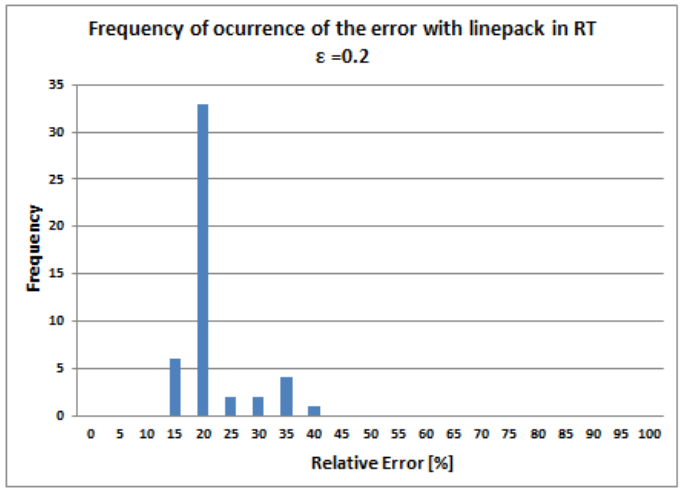

Figure A.8: Solution check of the CC-OPF in the RT stage with $\epsilon = 0.2$. Error = 3.09 %.

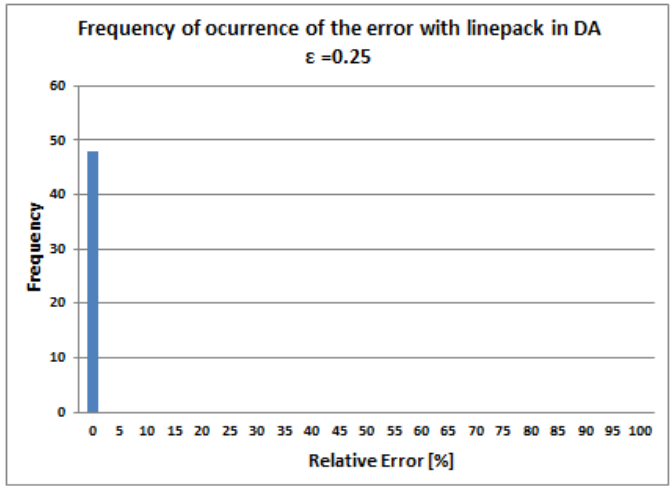

Figure A.9: Solution check of the CC-OPF in the DA stage with $\epsilon = 0.25$. Error = $1.67 \cdot 10^{-5}$%.

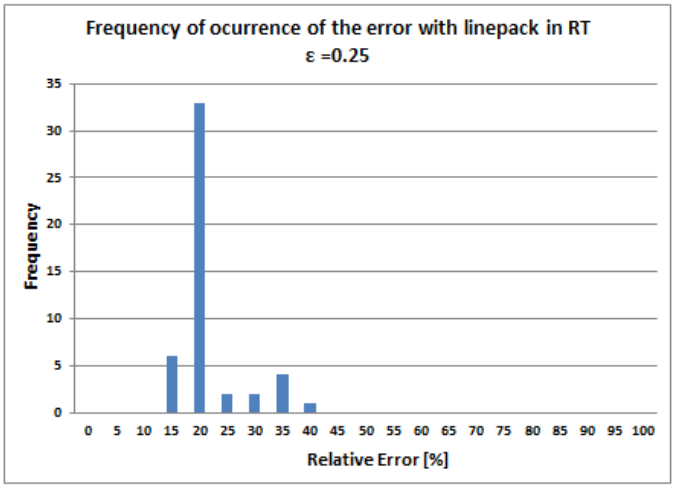

Figure A.10: Solution check of the CC-OPF in the RT stage with $\epsilon = 0.25$. Error $= 3.06$ %.

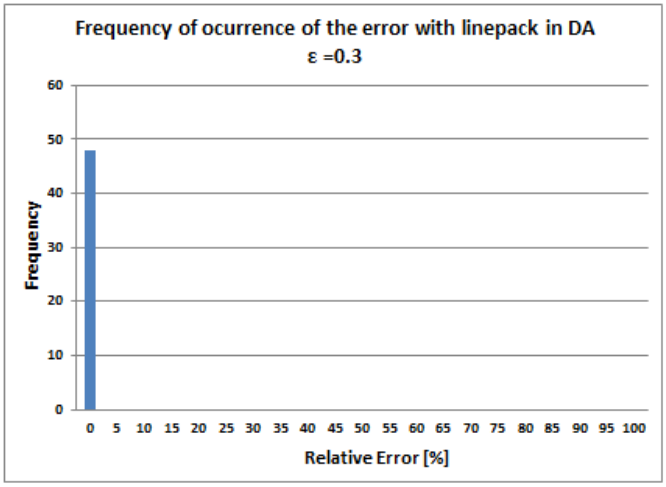

Figure A.11: Solution check of the CC-OPF in the DA stage with $\epsilon = 0.3$. Error $= 10^{-7}$%.

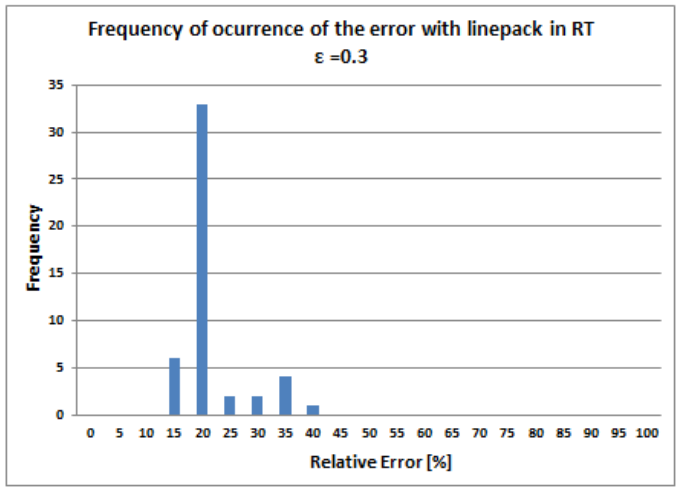

Figure A.12: Solution check of the CC-OPF in the RT stage with $\epsilon = 0.3$. Error $=2.81\%$.

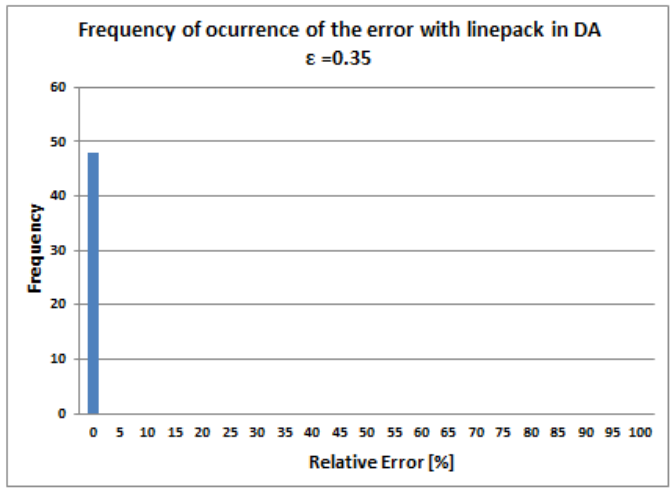

Figure A.13: Solution check of the CC-OPF in the DA stage with $\epsilon = 0.35$. Error $=10^{-7}\%$.

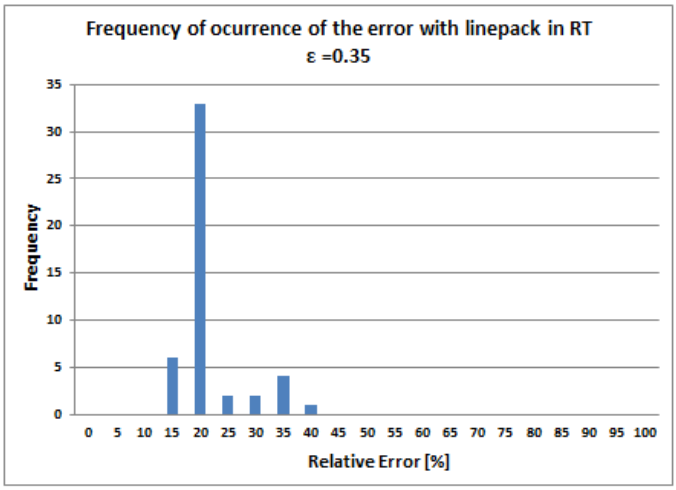

Figure A.14: Solution check of the CC-OPF in the RT stage with $\epsilon = 0.35$. Error $=2.82$ %.

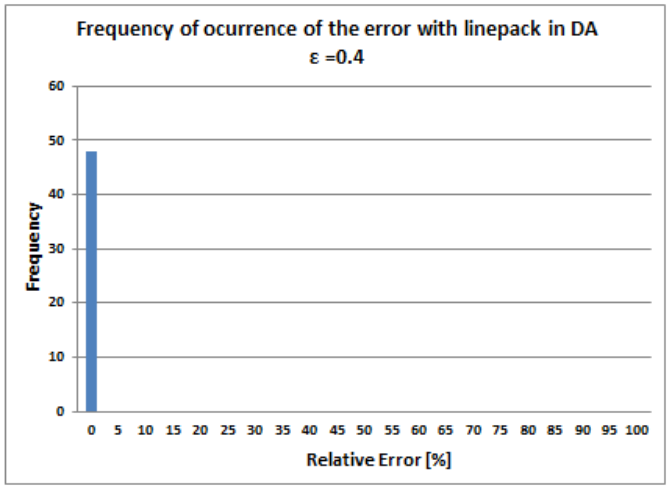

Figure A.15: Solution check of the CC-OPF in the DA stage with $\epsilon = 0.4$. Error $=2.00 \cdot 10^{-7}$%.

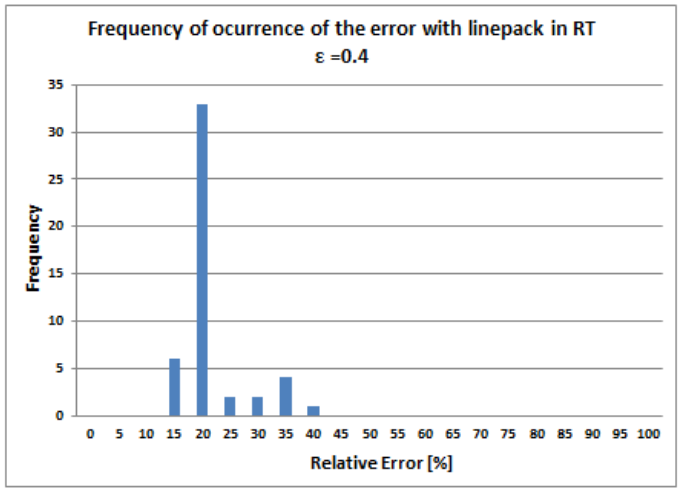

Figure A.16: Solution check of the CC-OPF in the RT stage with $\epsilon = 0.4$. Error $=2.83$ %.

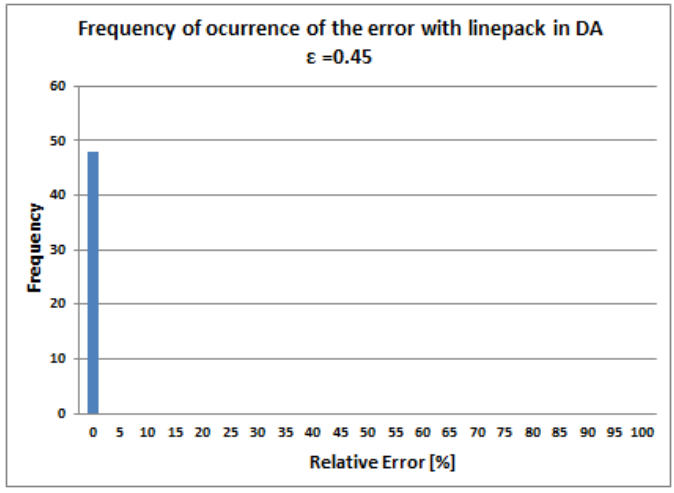

Figure A.17: Solution check of the CC-OPF in the DA stage with $\epsilon = 0.45$. Error $=10^{-7}$%.

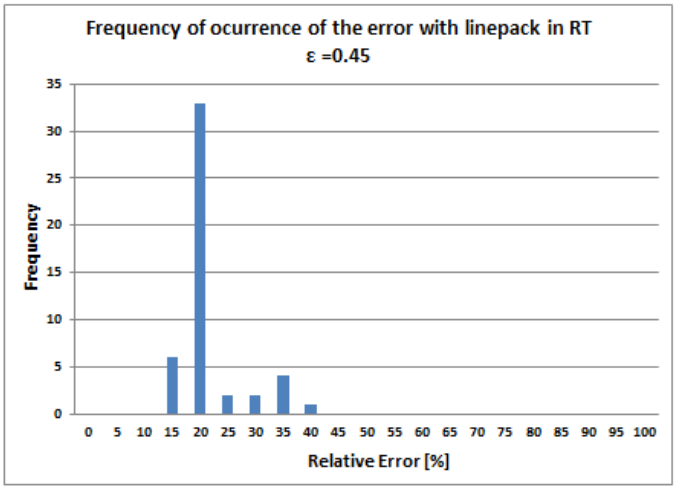

Figure A.18: Solution check of the CC-OPF in the RT stage with $\epsilon = 0.45$. Error $=2.91$ %.

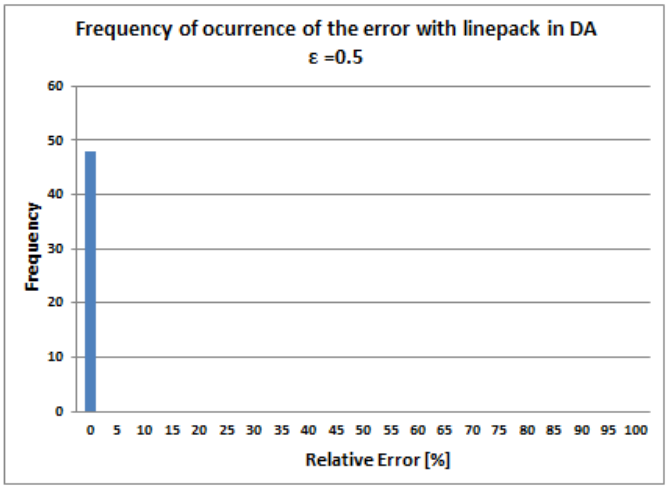

Figure A.19: Solution check of the CC-OPF in the DA stage with $\epsilon = 0.5$. Error $=10^{-7}$%.

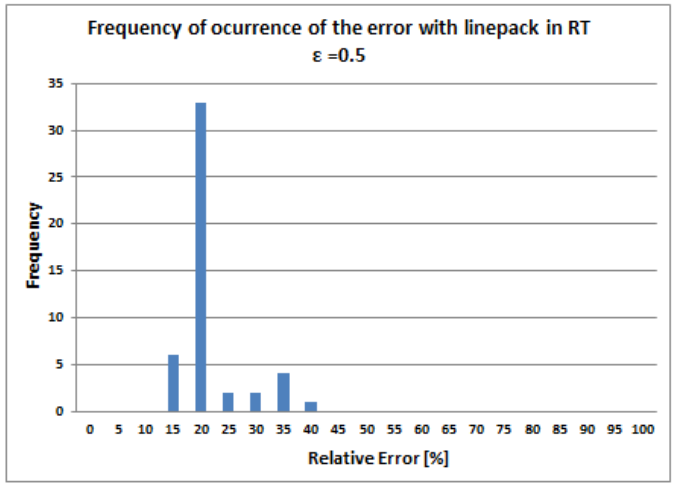

Figure A.20: Solution check of the CC-OPF in the RT stage with $\epsilon = 0.5$. Error =2.80 %.

APPENDIX B

Base case data

	NODAL INFORMATION											
	Type Power Supply	Cap [MW]	Conv Factor	Cost of Elec [$/MW]	Wind Farms	Wind Farms Cap [MW]	Gas Supply	Cap [kcf]	Elec Dem share	NG Demand share	Min Pr	Max Pr
N1	GFPP	152	12.65	-	Yes	500	-	-	0.33	0	100	500
N2	TPP	400	-	44.55	Yes	1000	-	-	0.33	0.9	100	500
N3	GFPP	155	14.88	-	-	-	Yes	15,000	0.33	0.1	100	500

Table B.1: Operational Characteristics of generators.

	LINES / PIPELINES INFORMATION					
	LINES		PIPELINES			
	Susceptance [S]	Cap [MW]	Kmu [kcf/psig]	$\Gamma_{m,u}$	S [kcf/(psig h)]	Initial Linepack
1-2	0.0146	175	28	1.1	121	39300
2-3	0.2253	175	-	-	-	-
3-1	0.0907	500	28	1	150	49300

Table B.2: Transmission line and pipeline characteristics.

	Wind Factor		**Electricity Demand [MW]**	**Natural Gas Demand [kcf]**
	Node 1	*Node 2*		
t1	0.80	0.90	708.73	7000
t2	0.90	0.85	602.63	6700
t3	0.85	0.75	1073.98	6400
t4	0.60	0.70	1030.90	6500
t5	0.70	0.80	851.00	6600
t6	0.68	0.58	582.04	6700
t7	0.50	0.56	378.60	7750
t8	0.30	0.40	944.03	7800
t9	0.45	0.20	1061.77	8550
t10	0.50	0.35	602.58	8700
t11	0.60	0.35	741.14	8700
t12	0.30	0.40	235.38	8550
t13	0.20	0.25	482.55	8550
t14	0.40	0.30	367.35	8550
t15	0.35	0.25	541.30	8400
t16	0.65	0.70	675.31	8550
t17	0.50	0.20	497.63	9000
t18	0.25	0.10	715.35	9000
t19	0.10	0.15	579.81	9000
t20	0.20	0.15	489.47	8700
t21	0.15	0.10	500.00	8250
t22	0.15	0.10	613.75	7500
t23	0.10	0.20	610.42	6600
t24	0.05	0.10	537.59	6700

Table B.3: Inputs of the wind factor, electricity and natural gas demands over 24 hour horizon.

Bibliography

[AG03] F. Alizadeh and D. Goldfarb. "Second-order cone programming". In: *Mathematical Programming* 95.1 (January 2003), pages 3–51. ISSN: 1436-4646. DOI: 10.1007/s10107-002-0339-5. URL: https://doi.org/10.1007/s10107-002-0339-5.

[Arv+13] Øystein Arvesen et al. "Linepack storage valuation under price uncertainty". In: *Energy* 52 (2013), pages 155–164.

[BCH12] Daniel Bienstock, Michael Chertkov, and Sean Harnett. *Chance Constrained Optimal Power Flow: Risk-Aware Network Control under Uncertainty*. 2012.

[Bee17] Nelson HF Beebe. *The Mathematical-Function Computation Handbook*. Springer, 2017.

[Che+19] Sheng Chen et al. "Unit Commitment with an Enhanced Natural Gas-Flow Model". In: *IEEE Transactions on Power Systems* (2019).

[CKA11] Spyros Chatzivasileiadis, Thilo Krause, and Göran Andersson. "Flexible AC Transmission Systems (FACTS) and power system security—A valuation framework". In: *2011 IEEE Power and Energy Society General Meeting*. IEEE. 2011, pages 1–8.

[Com12] European Commission. *Energy roadmap 2050*. Publications Office of the European Union, 2012.

[Due+14] Pablo Dueñas et al. "Gas–electricity coordination in competitive markets under renewable energy uncertainty". In: *IEEE Transactions on Power Systems* 30.1 (2014), pages 123–131.

[Göt+11] Manuel Götz et al. "Storage of volatile renewable energy in the gas grid applying 3-phase methanation". In: *Proceeding of International Gas Union Research Conference, l.-Seoul, République de Corée*. 2011.

[Göt+16] Manuel Götz et al. “Renewable Power-to-Gas: A technological and economic review”. In: *Renewable energy* 85 (2016), pages 1371–1390.

[Gur19] LLC Gurobi Optimization. *Gurobi Optimizer Reference Manual*. 2019. URL: `http://www.gurobi.com`.

[MBT09] Kjetil T Midthun, Mette Bjørndal, and Asgeir Tomasgard. “Modeling optimal economic dispatch and system effects in natural gas networks”. In: *The Energy Journal* (2009), pages 155–180.

[McC76] Garth P McCormick. “Computability of global solutions to factorable nonconvex programs: Part I—Convex underestimating problems”. In: *Mathematical programming* 10.1 (1976), pages 147–175.

[MP06] Wolfgang Marquardt and Costas Pantelides. *16th European Symposium on Computer Aided Process Engineering and 9th International Symposium on Process Systems Engineering*. Volume 21. Elsevier, 2006.

[NS06] Arkadi Nemirovski and Alexander Shapiro. “Convex approximations of chance constrained programs”. In: *SIAM Journal on Optimization* 17.4 (2006), pages 969–996.

[OPM19] Christos Ordoudis, Pierre Pinson, and Juan M Morales. “An integrated market for electricity and natural gas systems with stochastic power producers”. In: *European Journal of Operational Research* 272.2 (2019), pages 642–654.

[Ord18] Christos Ordouis. *Robust approaches for market clearing*. Large-scale optimization problems in energy systems: applications of decomposition techniques. 2018.

[Pin+17] Pierre Pinson et al. “Towards fully renewable energy systems: Experience and trends in Denmark”. In: *CSEE journal of power and energy systems* 3.1 (2017), pages 26–35.

[RMS17] Mariusz Ruszel, Tomasz Młynarski, and Adam Szurlej. *Energy Policy Transition: The Perspective of Different States*. Ignacy Lukasiewicz Energy Policy Institute, 2017.

[Roa16] Line A Roald. “Optimization methods to manage uncertainty and risk in power systems operation”. PhD thesis. ETH Zurich, 2016.

[Rub+08] R Rubio et al. “Integrated natural gas and electricity market: A survey of the state of the art in operation planning and market issues”. In: *2008 IEEE/PES Transmission and Distribution Conference and Exposition: Latin America*. IEEE. 2008, pages 1–8.

[Sch+19] Anna Schwele et al. “Coordination of Power and Natural Gas Systems: Convexification Approaches for Linepack Modeling”. English. In: *Proceedings of IEEE PES PowerTech 2019*. IEEE, 2019.

[Sch18] Anna Schwele. *aschwele/CoordPowerNG$_C$onvexLinepack : Electroniccompanion : CoordinationofPowerandNaturalGasSystems : ConvexificationApproachesforLi* December 2018. DOI: 10.5281/zenodo.2205984. URL: https://doi.org/10.5281/zenodo.2205984.

[She+18] Chen Sheng et al. *Unit Commitment of Integrated Electric and Gas Systems with an Enhanced Second-Order Cone Gas Flow Model*. Unit Commitment of Integrated Electric and Gas Systems with an Enhanced Second-Order Cone Gas Flow Model. 2018.

[Tra+18] Trung Hieu Tran et al. “Linepack planning models for gas transmission network under uncertainty”. In: *European Journal of Operational Research* 268.2 (2018), pages 688–702.

[ULD07] Clodomiro Unsihuay, JW Marangon Lima, and AC Zambroni De Souza. “Modeling the integrated natural gas and electricity optimal power flow”. In: *2007 IEEE Power Engineering Society General Meeting*. IEEE. 2007, pages 1–7.

[Vra+13a] Maria Vrakopoulou et al. “A Probabilistic Framework for Reserve Scheduling and N-1 Security Assessment of Systems With High Wind Power Penetration”. In: *IEEE Transactions on Power Systems* 28.4 (2013), pages 3885–3896.

[Vra+13b] Maria Vrakopoulou et al. “Probabilistic guarantees for the N-1 security of systems with wind power generation”. In: *Reliability and risk evaluation of wind integrated power systems*. Springer, 2013, pages 59–73.

[WWS13] Allen J Wood, Bruce F Wollenberg, and Gerald B Sheblé. *Power generation, operation, and control*. John Wiley & Sons, 2013.

[Zlo+17] AV Zlotnik et al. “Grid architecture at the gas-electric interface”. In: *Los Alamos Natl. Lab., Santa Fe, NM, USA, Rep. LA-UR-17-23662* (2017).

{2.7182818284}ϑφερτυθιοπσδφγηξκλ